II. PLASMA DYNAMICS

Prof. W. P. Allis	Prof. D. J. Rose	Prof. L. D. Smullin
Prof. S. C. Brown	Prof. A. H. Shapiro	Prof. J. B. Wiesner

RESEARCH OBJECTIVES

This heading covers all of the work that is supported in part by the National Science Foundation and is under the over-all supervision of the Plasma Dynamics Committee of the Massachusetts Institute of Technology. The general objective is to combine the technical knowledge of several departments, in a broad attempt to understand electrical plasmas, to control them, and to apply them to the needs of communication, propulsion, power conversion, and thermonuclear processes.

II-A. PLASMA PHYSICS*

Prof. S. C. Brown	Dr. J. L. Hirshfield	W. L. Jones
Prof. W. P. Allis	V. Arunasalam	W. R. Kittredge
Prof. D. J. Rose	C. D. Buntschuh	J. J. McCarthy
Prof. D. R. Whitehouse	J. D. Coccoli	W. J. Mulligan
Dr. G. Bekefi	E. W. Fitzgerald, Jr.	J. J. Nolan, Jr.
Dr. B. Brandt	S. Frankenthal	K-F. Voyenli
Dr. S. Gruber	P. J. Freyheit	R. E. Whitney

RESEARCH OBJECTIVES

The aim of this group continues to be the study of the fundamental properties of plasmas with more and more emphasis on high-density plasmas and plasmas in magnetic fields. To carry out this general objective, we have spent a great deal of effort on the production of plasmas of high-percentage ionization at low pressures under steady-state conditions, the achievement of which will allow us to carry on the fundamental studies in which we are most interested. At the present time, we have begun to achieve plasmas with high-percentage ionization by means of cesium plasmas, and we have several other schemes under way for producing them.

We are also studying ways of determining the characteristics of plasmas by means of microwaves and infrared interferometric methods. Along with these production and diagnostic studies, we are continuing measurements on the fundamental physics studies of loss and gain mechanisms of electrons in plasmas in magnetic fields. Considerable emphasis is being placed on studying the microwave radiation from plasmas, with and without magnetic fields, both as a tool for measuring the plasma temperature and thermal properties and as a means of understanding more about the motion of electrons and ions in magnetic fields.

Theoretical work has been concentrated on the study of waves in plasmas and of statistical theories of the nature of a plasma.

S. C. Brown

1. PLASMA TURBULENCE

Considerable theoretical effort on turbulence in plasmas has led to a program of experimental investigation. We think that if one were to break down a turbulent gas the

*This work was supported in part by the Atomic Energy Commission under Contract AT(30-1)-1842; in part by Air Force Cambridge Research Center under Contract AF19(604)-5992; and in part by National Science Foundation under Grant G-9330.

ions would follow the random component of the gas velocity. Since in turbulence local changes in the gas particle density take place, we would expect to find such an effect in the ions. If the electrons were to remain uniformly distributed throughout the discharge, large space-charge fields would build up. The electrons would then be accelerated toward regions of excess ions and away from regions of reduced ion density. In effect, the electrons will be forced to follow the turbulence through the effect of the ions.

Inlet and exhaust nozzles were built to produce a supersonic gas flow in a test section at static gas pressures in the 1-10 mm Hg region. The test section had a rectangular cross section of approximately 6 square inches. On the upstream side of the test section, provision was made for accepting various rectangular wire meshes. Downstream of the mesh a dc discharge was produced between two parallel water-cooled, square, stainless-steel plates of dimension 1.5 inches on a side. Measurements were taken of the current to Langmuir probes that consisted of platinum balls, approximately 22 mils in diameter, at the end of 2-mil tungsten wire approximately 4 mm in length. Three types of measurement were made:

(a) Static probe curves were taken of the average probe current versus the dc probe voltage. (The voltage was measured with respect to the positive discharge plate.)

(b) The integrated power spectrum of the time-variant component of the probe current was measured. That is, the power in current fluctuations was measured for a

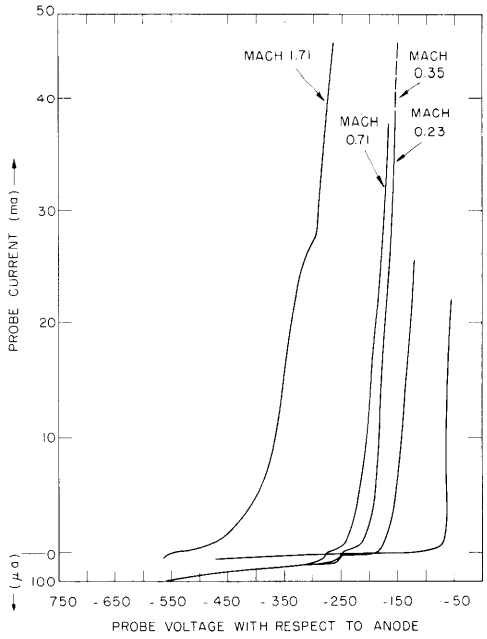

Fig. II-1. Static probe curves with Mach number as the parameter.

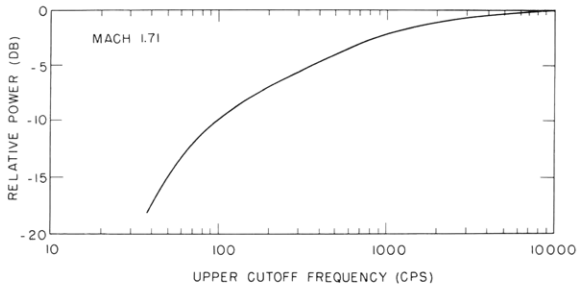

Fig. II-2. Integrated power spectrum.

fixed lower cutoff frequency of a continuously variable filter versus the filter's upper cutoff frequency.

(c) Correlation studies of the fluctuating currents in the two probes as a function of their spatial separation were made.

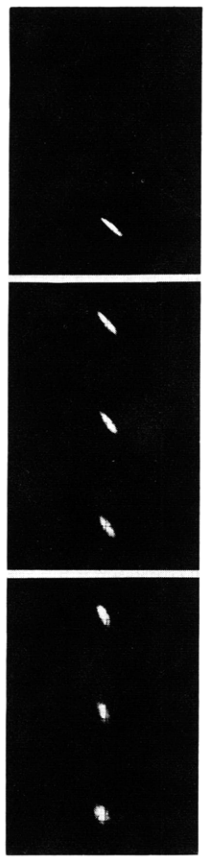

Fig. II-3. Oscilloscope correlation patterns. The spacing between probes increases from top to bottom of the figure.

For all measurements, the discharge static pressure was in the neighborhood of 4 mm Hg, and the velocity was varied from no-flow up to Mach 1.71. During these preliminary measurements use was made of a sheet of steel with perforations 0.25 inch in diameter instead of the wire meshes, since we hoped that this would produce a strong turbulence-producing discontinuity. Figure II-1 gives the static probe curves with Mach number as the parameter. Figure II-2 is a typical measurement of the integrated power spectrum. The effect of Mach number here was to increase the power in the fluctuations but not to vary the general shape of the spectrum significantly.

During these first measurements, the correlations were indicated by the shape of a pattern produced on the screen of an oscilloscope whose x-axis deflection was produced by one of the probe pair and the y-axis deflection by the other. A 45° line indicates perfectly correlated probe currents, and a large white dot indicates

total lack of correlation. Photographs were taken of the oscilloscope pattern for each probe separation. Figure II-3 illustrates these measurements.

Fluctuations in the probe current were observed when there was no mesh in place and the gas was flowing. These fluctuations produced good correlation for all possible probe separations. For this reason, we think that wall turbulence caused fluctuations in the sheath at the positive discharge electrode that was used as a reference. This wall turbulence is thought to exist even with the turbulence-producing steel sheet in position and would account for greater correlation in the probe-current fluctuations than would be expected from the mesh turbulence.

Modifications of the experiment are in progress and will soon be tried. We hope that some of the difficulties encountered in this first attempt will be eliminated.

S. Gruber, G. Bekefi

2. CYCLOTRON EMISSION FROM PLASMAS WITH NON-MAXWELLIAN DISTRIBUTIONS

In Quarterly Progress Report No. 59 (page 3) we outlined a method of computing the emission from a plasma with a non-Maxwellian distribution of electron energies, $f(\epsilon)$. Here we apply the method to the case in which the emission takes place as a result of the orbital motion of energetic electrons in a uniform external magnetic field.

A single electron of total energy (rest plus kinetic) ϵ radiates in an infinite set of harmonics, n, of its orbital frequency. The rate of emission $j_\omega^{(1,2)}$ is given by

$$j_\omega^{(1,2)}(\epsilon) = \frac{e^2\omega^2}{8\pi^2\epsilon_o c} \sum_1^\infty A_n^{(1,2)} \delta\left[\left(n\omega_b mc^2/\epsilon\right)-\omega\right] \tag{1}$$

Here the numerals 1, 2 refer to the polarization of the electric vector parallel and perpendicular to the applied magnetic field B, respectively; A_n is a dimensionless parameter that represents the strength of the radiation, and $\omega_b = eB/m$, where m is the "rest mass" of the electron.

We consider a uniform slab of plasma of thickness L, immersed in a magnetic field that is applied parallel to the faces of the slab. The emission occurs mainly in a narrow cone oriented at 90° to the magnetic field; the higher the harmonic number, the narrower the cone. The radiation intensity I_ω, in the radian frequency interval $d\omega$, which escapes normally from the surface of the slab (we neglect all other angles of emission) is given by

$$I_\omega^{(1,2)} = B^{(1,2)}(\omega, T_r)\left[1-\exp\left(-\alpha_\omega^{(1,2)}L\right)\right] \tag{2}$$

where $B(\omega, T_r)$ is the equilibrium, black-body intensity (1),

$$B^{(1,2)}(\omega,T_r) = \frac{\omega^2}{8\pi^3 c^2}\left[-\frac{\int j_\omega^{(1,2)}(\epsilon)\, f(\epsilon)\, \epsilon[\epsilon^2-(mc^2)^2]^{1/2}\, d\epsilon}{\int j_\omega^{(1,2)}(\epsilon)[\partial f/\partial\epsilon]\, \epsilon[\epsilon^2-(mc^2)^2]^{1/2}\, d\epsilon}\right] \tag{3}$$

The bracketed term of Eq. 3 defines the radiation temperature (T_r), which for a Maxwellian distribution becomes the electron temperature (T). The parameter $a_\omega^{(1,2)}$ of Eq. 2 is the absorption coefficient of the plasma given by

$$a_\omega^{(1,2)} = -\frac{32\pi^4 N}{\omega^2 c}\int j_\omega^{(1,2)}[\partial f/\partial\epsilon]\, \epsilon[\epsilon^2-(mc^2)^2]^{1/2}\, d\epsilon \tag{4}$$

Here, N is the electron concentration, and $f(\epsilon)$ is assumed, in these calculations, to be spherically symmetrical in velocity space and normalized, so that

$$\frac{4\pi}{c^3}\int f(\epsilon)\, \epsilon[\epsilon^2-(mc^2)^2]^{1/2}\, d\epsilon = 1 \tag{5}$$

Equations 1-5 allow us to evaluate the radiation intensity I_ω per unit surface area of the plasma slab. Difficulties arise unless the strength function A_n of Eq. 1 is simplified by suitable approximations (2). For electron energies less than approximately 100 kev the following approximations were used: At low harmonic numbers ($n = \omega/\omega_b < 3$), the radiation from successive harmonics overlaps to a negligible degree, and the summation in Eq. 1 need not be performed. Also, contributions to j_ω from waves polarized along the magnetic field can be neglected with the result that

$$\begin{aligned} A_n^{(1)} &= 0 \\ A_\omega^{(2)} &= \frac{n^{2n}}{(2n+1)!}\left[1-\left(\frac{mc^2}{\epsilon}\right)^2\right]^n \end{aligned} \tag{6}$$

At harmonic numbers greater than approximately 3, overlapping of harmonics can be very pronounced, and in this frequency range a good approximation for A_ω is

$$\begin{aligned} A_n^{(1)} &= 0 \\ A_n^{(2)} &= \left(\frac{mc^2}{\epsilon}\right)^{1/2}\frac{\exp[2n\, mc^2/\epsilon]}{4(\pi n^3)^{1/2}}\left[\frac{\epsilon - mc^2}{\epsilon + mc^2}\right]^n \end{aligned} \tag{7}$$

The magnitude and spectrum of the cyclotron emission fall into two distinct classes, according to the energy dependence of the distribution function $f(\epsilon)$. If $f(\epsilon)$ decreases everywhere monotonically with increasing ϵ (that is, $\partial f(\epsilon)/\partial\epsilon < 0$), then the general

characteristics of I_ω do not differ greatly from those when $f(\epsilon)$ is a Maxwellian distribution. However, when $f(\epsilon)$ has at least one maximum displaced from $\epsilon = 0$, (that is, $\partial f(\epsilon)/\partial \epsilon > 0$ somewhere in the energy range), then a_ω and $B(\omega, T_r)$ become negative at certain frequencies. Instead of being attenuated in its passage through the plasma, the radiation grows, with the result that I_ω can exceed black-body emission by many orders of magnitude. If the growth is too excessive, nonlinear effects can set in and cause the plasma to become unstable. This amplification process is not confined to cyclotron emission alone; it can also occur for other emission processes. In the case of cyclotron emission, it is a relativistic effect and will not take place if computations are made in the limit, when terms of order $(v/c)^2$ are neglected.

a. Emission for Distribution Functions $\partial f/\partial \epsilon < 0$

We assume distribution functions of the form

$$f(\beta) = \exp(-b\beta^{\ell}) \tag{8}$$

where $\beta = v/c$ and ℓ and b are positive constants; $\ell = 2$ represents a Maxwellian distribution of a given mean energy $\bar{u}$, whose magnitude determines the value of b; $\ell < 2$ implies that there is an excess of energetic electrons in the tail of the distribution, as compared with a Maxwellian distribution of the same mean energy, $\bar{u}$. The opposite is true when $\ell > 2$.

The frequency spectrum of cyclotron emission has the following characteristics: for frequencies ω smaller than some characteristic frequency ω^*, self-absorption of the radiation is large ($a_\omega L$ of Eq. 2 is greater than 1) and the intensity I_ω approaches the equilibrium intensity $B(\omega, T_r)$; the harmonics are, so to speak, trapped in the black-body continuum. For frequencies $\omega \gg \omega^*$ self-absorption can be neglected, and the

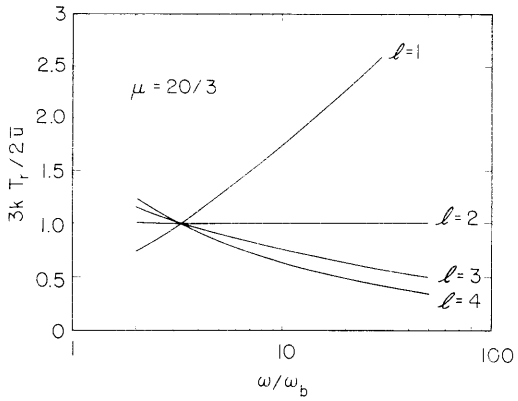

Fig. II-4. The radiation temperature T_r as a function of frequency for various distribution functions $f \propto \exp(-b\beta^{\ell})$.

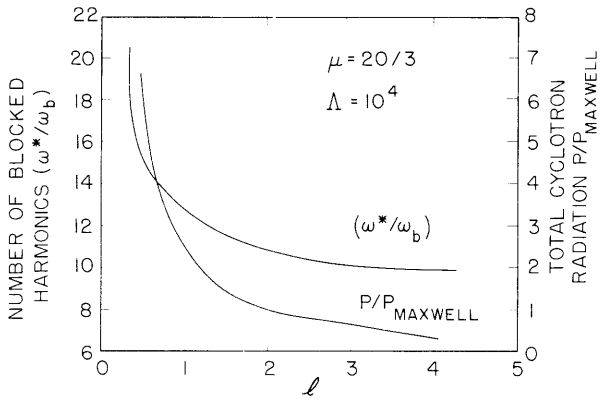

Fig. II-5. The number of harmonics ω^* trapped in the black-body continuum and the total cyclotron emission (normalized to the emission from a Maxwellian plasma) as a function of the distribution of electron velocities, $f \propto \exp(-b\beta^{\ell})$.

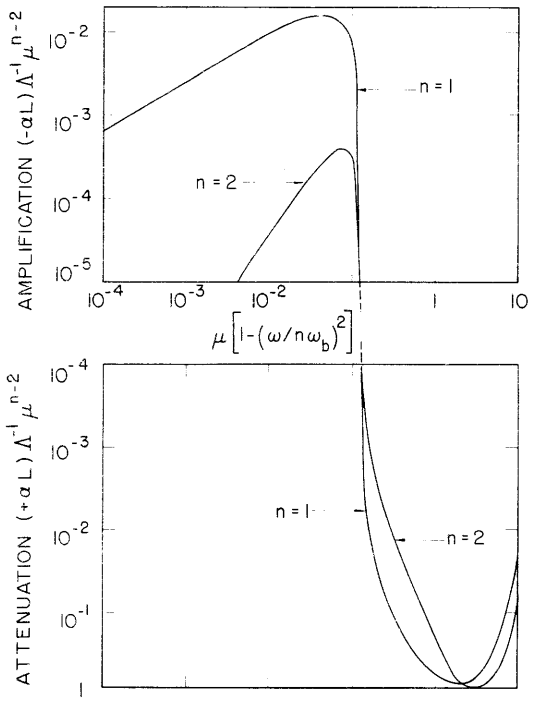

Fig. II-6. The transition from a positive to a negative absorption coefficient, with varying frequency, for the first two harmonics. The plot is for a distribution function $f \propto \beta^p \exp(-b\beta^2)$, with $p = 0.2$.

radiation in these harmonics leaves the plasma unhindered. The dividing line between the two regimes of emission is generally defined by

$$a(\omega = \omega^*)\, L = 1 \tag{9}$$

In computing the total cyclotron emission over all frequencies, not too great an error is committed by neglecting radiation at frequencies $\omega > \omega^*$. We make this approximation in the present calculations.

To find the total emission, we must first calculate the spectral distribution of $B(\omega, T_r)$ from Eq. 3. Figure II-4 shows the variation of the radiation temperature (T_r) (defined by the bracketed term of Eq. 3), for different values of ℓ of the distribution function, Eq. 8.

Calculations of the absorption coefficient a_ω from Eq. 4 and use of Eq. 9 yields the critical frequency ω^*. We assume that the plasma has the following properties: $\mu \equiv mc^2/\bar{u}$ equal to 20/3, which implies an equivalent electron temperature ($T \equiv (2/3)\bar{u}$) of 50 kev. The dimensionless parameter $\Lambda \equiv \left[\omega_p^2 L / \omega_b c\right]$, which specifies the electron density, the size of the plasma, and the magnetic field strength, was chosen to be 10^4. This means that when L = 1 meter and B = 10^4 gauss, the electron density is approximately 10^{14} cm^{-3}, and the outward kinetic pressure of the charged particles is nearly balanced by the inward magnetic pressure; that is, $2NkT = B^2/2\mu_o$.

Figure II-5 shows the number of harmonics trapped in the black-body continuum with change in the distribution function. The frequency ω^* changes little for small departures of the distribution function from a Maxwellian distribution. Only when ℓ becomes much smaller than 2, does ω^* increase very drastically. The total emission is obtained by integrating Eq. 2 over all frequencies between $\omega = 0$ and $\omega = \omega^*$. This emission, normalized to the emission from a Maxwellian plasma, is also shown in Fig. II-5. From these results we conclude that when $\partial f/\partial \epsilon < 0$, small departures of the distribution function from a Maxwell distribution do not seriously affect the net cyclotron emission.

b. Emission for Distribution Functions $\partial f/\partial \epsilon > 0$

Here we assume distribution functions of the form

$$f(\beta) = \beta^p \exp(-b\beta^2) \qquad p \geq 0 \tag{10}$$

When p = 0, the distribution is Maxwellian; when $p \neq 0$, the distribution function is peaked at some energy $\epsilon \neq 0$. If the mean energy $\bar{u}$ is kept fixed, the spike in the distribution function becomes narrower and narrower, the larger the value of p.

The spiked distribution functions cause the absorption coefficient a_ω to take on negative values (that is, the wave amplifies) in narrow frequency ranges near the maxima of the harmonics of the cyclotron frequency. Outside these frequency ranges the wave attenuates in the normal way. Figure II-6 illustrates this effect for the first two

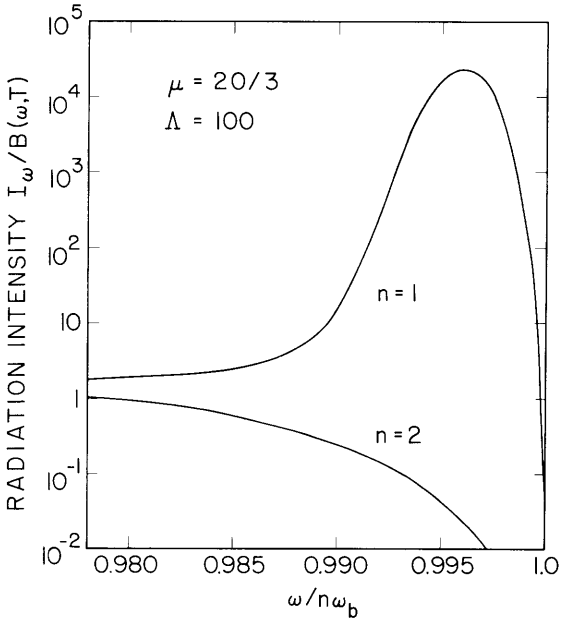

Fig. II-7. The radiation intensity normalized to $B(\omega, T) = (2\bar{u}\omega^2/24\pi^3c^2)$ as a function of frequency. Amplification occurs for the first harmonic n = 1, and no amplification occurs for n = 2 (p=0. 2).

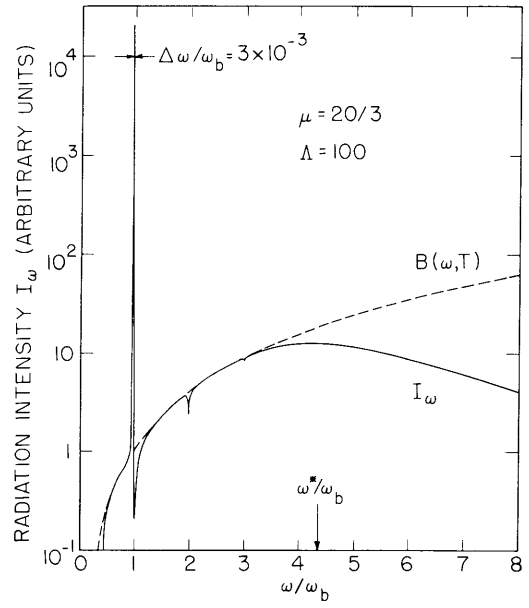

Fig. II-8. Complete view of the emission spectrum with the large peak at $\omega = \omega_b$ (p=0. 2).

harmonics. In these calculations we take p = 0.2. Despite this relatively small perturbation of the Maxwellian distribution, the amplification of the radiation $\alpha_\omega L$ is appreciable, and the actual intensity I_ω greatly exceeds the black-body emission of a Maxwellian plasma.

Figure II-7 illustrates the intensity of emission I_ω as a function of frequency for the first two harmonics, with p = 0.2. The intensity is normalized to the black-body intensity that would exist for a Maxwellian distribution of the same mean energy ($\bar{u} = 20/3$). The peak intensity increases with increasing electron density, and hence with increasing Λ. However, we have purposely chosen a small value of $\Lambda = 10^2$ (when L = 1 meter and $B = 10^4$ gauss, $N \approx 10^{12}$ electrons per cc) to ensure that for the frequencies that are of interest, $\omega \approx \omega_b, 2\omega_b, \ldots$, the plasma frequency $\omega_p \ll \omega$. The reason is that the theory presented here (Eqs. 2, 3, 4) is strictly valid only for tenuous plasmas with $\omega_p/\omega < 1$.

Figure II-8 illustrates the over-all frequency spectrum. We note the large peaks superimposed on the black-body continuum and the frequency ω^* at which the radiation ceases to be black. Despite the narrowness of the emission spikes (the half power width $\nabla\omega$ of the first harmonic is $10^{-3}\omega_b$), the total emission under the first spike alone (n=1) is greater than the integrated black-body emission between frequencies $\omega = 0$ and $\omega = \omega^*$. This radiation, therefore, plays an important part in estimating the total radiation loss from thermonuclear devices.

The amplification mechanism discussed does not occur when the radiation from individual harmonics overlaps strongly and thus causes the emission to be a continuous smooth function of ω. Overlapping is prevalent at higher harmonic numbers and is particularly pronounced in the emission from highly relativistic electrons; that is, unless the distribution function $f(\epsilon)$ has a very sharp spike in energy. When this is so, the radiation from each harmonic can be considered as a separate entity, and amplification of the radiation can take place. For overlapping to be small, the half-power width $\Delta\epsilon$ in the energy distribution of electrons must be small compared with the separation between harmonics; that is,

$$\Delta\epsilon \ll \epsilon(\omega_b/\omega) \tag{11}$$

For emission from highly relativistic electrons ($\epsilon \gg mc^2$), the harmonics are most intense in the vicinity of $n = (\epsilon/mc^2)^3$. It is this frequency range that is of greatest interest when attempting to interpret the nonthermal emission from radio sources in terms of cyclotron emission. For amplification of the radiation to occur at these frequencies (as has been suggested), would require the existence of spikes in the energy distribution of half widths

$$\Delta\epsilon \approx \epsilon(mc^2/\epsilon)^3$$

With electron energies of 500 mev, $(\nabla\epsilon/\epsilon) \approx 10^{-9}$. The existence of such almost monoenergetic electron "beams" in interstellar space is probably unlikely, and amplification of cyclotron radiation will not occur.

G. Bekefi, J. L. Hirshfield

References

1. G. Bekefi and J. L. Hirshfield, Radiation from plasmas with non-Maxwellian distributions, Quarterly Progress Report No. 59, Research Laboratory of Electronics, M. I. T., Oct. 15, 1960, p. 3.

2. B. A. Trubnikov (English translation of doctoral thesis, Moscow University), Report AEC-tr-4073, U. S. Atomic Energy Commission.

3. R. Q. Twiss, Australian J. Phys. 11, 564 (1958).

3. SYNCHROTRON RADIATION AND NEGATIVE ABSORPTION BY NONTHERMAL ELECTRONS IN A MAGNETIC FIELD

It has been pointed out by Twiss (1), and independently by Bekefi and Hirshfield (2), that under certain conditions electromagnetic radiation propagating through a nonthermal electron gas in the presence of a magnetic field may experience amplification. In particular, negative absorption may occur at frequencies near the peaks of the synchrotron emission spectrum if the electron energy distribution function has a maximum for some nonzero value of energy.

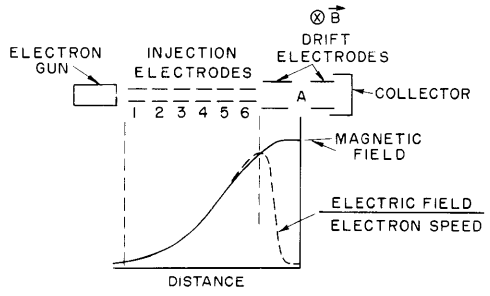

Fig. II-9. Injection of the electron beam into the magnetic field.

An experiment is in progress to detect this effect in an approximately monoenergetic electron beam. Since the synchrotron radiation is a relativistic effect, it is more easily detected as the electron energy is increased. Electrons with an energy of 1-2 kev transverse to a magnetic field of 1000 gauss, and with a density greater than 10^6 electrons per cubic centimeter, yield a third harmonic that is detectable by existing radiometric techniques.

Figure II-9 illustrates the manner in which the electrons are given the necessary transverse energy. The electron gun supplies a beam of electrons at the desired energy. The beam enters between injection electrodes, numbered 1 in Fig. II-9, located in a region of very low magnetic field strength. The electric field at the i^{th} electrode is approximately $E_i = vB_i$, where B_i is the magnetic field at the i^{th} electrode and v is the electron velocity. In this manner, the magnetic force is canceled by the

electric force as the electrons move into the region of high magnetic field strength. The electrons emerging from the final pair of injection electrodes enter the region of the drift electrodes where the electric field is greatly reduced, but the magnetic field is maximum. The electric force is much smaller than the magnetic force and the electrons attain a cyclotron motion. The small electric field is necessary to cause the electrons to drift past the region marked A in Fig. II-9 where microwave transmitting and receiving antennas can be located.

This scheme has been successful for injecting electrons of energies in the vicinity of 2 kev into magnetic fields of 900 gauss strength. An attempt will soon be made to detect and study the third harmonic of the synchrotron radiation, with the use of an X-band radiometer that is in the final stage of construction. Also, improvement of the shielding of the electron gun from the fringing magnetic field has been undertaken in order to inject electrons into stronger magnetic fields. This will make possible detection of the fundamental and second harmonics with the use of the X-band radiometer.

In a previous report (3) the contribution of magnetic-field gradients to the production of cyclotron frequency harmonics was examined. That analysis showed that in the present experiment the contribution of these effects will be negligible.

The negative absorption near the cyclotron frequency of the "transit-time" broadened emission spectrum of a mildly relativistic monoenergetic electron gas has been calculated. The absorption coefficient α for a plane polarized wave with its electric vector and direction of propagation both perpendicular to the steady magnetic field is

$$\alpha = \frac{\mathrm{Re}(\sigma_T)}{\epsilon_o \omega} \tag{1}$$

where, according to Allis and Buchsbaum (4),

$$\mathrm{Re}(\sigma_T) = -\frac{ne^2}{m}\frac{4\pi}{3}\int_0^\infty \mathrm{Re}\left\{\frac{\nu + j\omega}{(\nu+j\omega)^2 + \omega_b^2}\right\} v^3 \frac{\partial f_o^o}{\partial v}\, dv \tag{2}$$

and f_o^o is the undisturbed isotropic distribution function.

If it is assumed that $\omega \approx \omega_b$ and $\nu/\omega \ll 1$, then

$$\mathrm{Re}(\sigma_T) \approx -\frac{ne^2}{m}\frac{4\pi}{3}\int_0^\infty \frac{\nu v^3}{(\omega-\omega_b)^2 + \nu^2}\frac{\partial f_o^o}{\partial v}\, dv \tag{3}$$

or, upon integrating by parts,

$$\mathrm{Re}(\sigma_T) = \frac{ne^2}{m}\frac{4\pi}{3}\int_0^\infty f_o^o \frac{\partial}{\partial v}\left[\frac{\nu v^3}{(\omega-\omega_b)^2 + \nu^2}\right] dv \tag{4}$$

The condition for negative absorption is that

$$f_o^o \frac{\partial}{\partial v}\left[\frac{\nu v^3}{(\omega-\omega_b)^2+\nu^2}\right] < 0 \tag{5}$$

over a proper range of v to make the integral in Eq. 4 negative. For a very narrow distribution function, f_o^o, the condition is simply

$$\frac{\partial}{\partial v}\left[\frac{\nu v^3}{(\omega-\omega_b)^2+\nu^2}\right]\Bigg|_{v=v_o} < 0 \tag{6}$$

The distribution function f_o^o can be written $\propto \delta(v-v_o)$ merely to indicate that the width of the distribution function is so small that the term $\frac{\partial}{\partial v}\left[\frac{\nu v^3}{(\omega-\omega_b)^2+\nu^2}\right]$ is essentially constant over this range of v. This is mathematically convenient in evaluating Eq. 4,

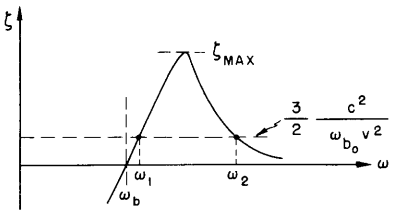

Fig. II-10. The function $\zeta(\omega)$.

but f_o^o cannot be rigorously set equal to $\delta(v-v_o)$ if the contribution to the Boltzmann equation of the higher spherical harmonic components of the distribution function are to be ignored.

For constant ν, inequality 6 becomes

$$\frac{\omega-\omega_b}{(\omega-\omega_b)^2+\nu^2} > \frac{3}{2}\frac{c^2}{\omega_{b_o} v^2} \tag{7}$$

where $\omega_b \approx \omega_{b_o}\left(1-\frac{1}{2}\frac{v^2}{c^2}\right)$, $\omega_{b_o} = \frac{e}{m}B$, and m is the electron rest mass.

Denote the left-hand side of inequality 7 ζ, then ζ has the qualitative behavior shown in Fig. II-10 for $\omega < \omega_b$, $\zeta < 0$; and for $\omega \gg \omega_b$, $\zeta \to \frac{1}{\omega} \to 0$.

The range of frequencies for which inequality 7 holds is given by replacing the inequality sign with an equal sign and finding the roots $(\omega-\omega_b)_{1,2}$:

$$(\omega-\omega_b)_{1,2} = \frac{\omega_{b_o} v^2}{3c^2} \pm \left[\left(\frac{\omega_{b_o} v^2}{3c^2}\right)^2 - \nu^2\right]^{1/2} \tag{8}$$

The condition for real roots is that

$$\nu < \frac{\omega_{b_o} v^2}{3c^2} \tag{9}$$

In the present experiment, ν is taken as a constant because the gas pressure is maintained so low ($p < 10^{-8}$ mm Hg[2]) that only the "transit time" of the electrons past the microwave antenna contributes to the broadening of the emission spectrum. The transit time in the drift region is determined by the drift velocity $v_d = E/B$ and is independent of the speed of the electrons, v. Some typical conditions are $v_d = 10^4$ meter/sec, $(v/c)^2 = 0.004$, $\omega_{b_o} = 1.76 \times 10^{10}$ rad/sec, antenna width L = 0.01 meter. Then $\left(\omega_{b_o} v^2\right)/3c^2 = 2.4 \times 10^7 \text{ sec}^{-1} > 7 \times 10^5 \text{ sec}^{-1} = \nu$, and $(1/2\pi)(\omega-\omega_b)_{1,2} = (0.0255, 7.45)$ mc. Also, $\nu/\omega = 4 \times 10^{-5} \ll 1$, $(1/2\pi)\left(\omega_{b_o} - \omega_b\right) = 40$ mc, and $\omega - \omega_b \ll \omega$ are compatible with the assumptions used to obtain Eq. 3.

From Eq. 8 we see that amplification occurs over a very narrow range of frequencies between the wider range from ω_b to ω_{b_o}.

If we set $f_o^o = \frac{3}{4\pi v_1^2}\delta(v-v_1)$, Eq. 4 becomes

$$\text{Re}(\sigma_T) = \frac{ne^2}{m} \frac{\nu}{(\omega-\omega_b)^2 + \nu^2}\left[1 - \frac{2}{3}\frac{v_1^2}{c^2}\omega_{b_o}\frac{(\omega-\omega_b)}{(\omega-\omega_b)^2+\nu^2}\right] \tag{10}$$

The minimum value of $\text{Re}(\sigma_T)$ occurs when ζ is a maximum; and it occurs when $\omega - \omega_b = \nu$. Thus

$$\text{Re}(\sigma_T)_{\min} = \frac{ne^2}{m}\frac{1}{2\nu}\left[1 - \frac{1}{3}\frac{v_1^2}{c^2}\frac{\omega_{b_o}}{\nu}\right] \tag{11}$$

Setting $n = 10^{14}$ electrons per cubic meter and utilizing the values of the parameters in the example given above yields $\alpha_{\min} \approx 500$. This is obviously incompatible with the assumption of small-signal theory involved in Eq. 1, and indicates the existence of an instability.

The analysis is strictly correct only for an electron gas with an isotropic velocity distribution. For an electron beam containing electrons in cyclotron motion, the distribution is certainly anisotropic in velocity space. However, the negative absorption

effect is probably more closely tied to the energy distribution than to the isotropy of this distribution, so that this analysis should yield the qualitative details; that is, for sharply peaked energy distribution of the electrons, negative absorption takes place over a narrow range of frequencies below and close to ω_{b_o}; this range decreases as ν increases; and it increases with ω_{b_o} and v/c. The amplitude increases with decreasing ν. The effect is relativistic in origin.

J. D. Coccoli

References

1. R. Q. Twiss, Australian J. Phys. 11, 564 (1958).

2. G. Bekefi, J. L. Hirshfield, and S. C. Brown, Kirchhoff's radiation law for plasmas with non-Maxwellian distributions (to be published in Phys. Fluids).

3. J. D. Coccoli, Harmonics of cyclotron radiation resulting from inhomogeneity of the magnetic field, Quarterly Progress Report No. 58, Research Laboratory of Electronics, M.I.T., July 15, 1960, p. 27.

4. W. P. Allis and S. J. Buchsbaum, Notes on Plasma Dynamics, Summer Session 1959, M.I.T., Sec. D-23.

4. LOCAL INSTABILITIES CAUSED BY PRESSURE ANISOTROPY IN A COLLISIONLESS PLASMA

a. Introduction

In an important class of plasma physics problems, notably those dealing with high-temperature, low-density plasmas, the binary collisions between the particles are unimportant, and the particles interact only through macroscopic electric and magnetic fields. A property of a plasma of this type is that the pressure tensor will generally be anisotropic. This will lead to certain types of instability that do not occur in an isotropic, collision-dominated plasma.

In dealing with the problem of magnetohydrodynamic, collision-free shock waves moving across a magnetic field, it is very natural to assume a purely two-dimensional dissipation mechanism in the structure region of the wave; that is, a dissipation mechanism in which the energy is dissipated only in the particle's two degrees of freedom perpendicular to the magnetic field. A dissipation mechanism of this type will lead to an anisotropic pressure behind the structure region. It follows from the general conservation equations for mass, momentum, and energy, that this anisotropy will grow without limits with increasing strength of the shock wave. It has therefore been suggested that certain types of instability associated with this anisotropy may play a part in the dissipation mechanism (1). In particular, this can be expected for strong shock waves, in which a strong anisotropy would be generated by a purely two-dimensional

dissipation mechanism. It is the purpose of this paper to investigate the conditions under which instabilities associated with the anisotropy in the pressure occur.

b. Collision-Free Magnetohydrodynamics: Energy Principle for Stability

We shall confine ourselves to magnetohydrodynamic instabilities of a certain type and investigate them through an energy principle (2). This energy principle is based upon a magnetohydrodynamic description of a collision-free plasma in the presence of a magnetic field. The description has been developed by several authors (2, 3). The governing equations will now be presented. The continuity equation is

$$\frac{d\rho}{dt} = -\rho \nabla \cdot \underline{v}$$

where d/dt is the substantial derivative, ρ is the density, and $\underline{v}$ is the velocity. The momentum equation is

$$\rho \frac{d\underline{v}}{dt} = -\nabla \cdot \underline{\underline{P}} + \underline{j} \times \underline{B}$$

where $\underline{\underline{P}}$ is the pressure tensor, $\underline{j}$ is the current density, and $\underline{B}$ is the magnetic field. The pressure tensor is of the form

$$\underline{\underline{P}} = p_{\parallel} \underline{e}\,\underline{e} + p_{\perp} (\underline{\underline{I}} - \underline{e}\,\underline{e})$$

where $\underline{e} = \underline{B}/B$ is a unit vector along B, and $\underline{\underline{I}}$ is a unit tensor. Two adiabatic equations for the pressure are:

$$\frac{dp_{\parallel}}{dt} = -p_{\parallel} \nabla \cdot \underline{v} - 2p_{\parallel}\, \underline{e} \cdot (\underline{e} \cdot \nabla \underline{v})$$

$$\frac{dp_{\perp}}{dt} = -2p_{\perp} \nabla \cdot \underline{v} + p_{\perp}\, \underline{e} \cdot (\underline{e} \cdot \nabla \underline{v})$$

The second of these equations expresses the conservation of magnetic moment of the particles, and the sum of the equations expresses adiabaticity. Ohm's law may be stated: $\underline{E} + \underline{v} \times \underline{B} = 0$. Maxwell's equations are used in their usual magnetohydrodynamic approximation: $\nabla \times \underline{E} = -\partial \underline{B}/\partial t$, $\nabla \times \underline{B} = \underline{j}$, $\nabla \cdot \underline{B} = 0$.

The conditions under which this description is valid are not completely known, but it is assumed that they are essentially the same as those for which the ordinary collision-dominated magnetohydrodynamics is valid, with the important change that the Larmor radius of the particles must now be assumed to be very much smaller than all other characteristic lengths in the plasma; in particular, smaller than the mean-free path of the particles.

As we have mentioned, an energy principle for the investigation of the stability of

static equilibrium states can be obtained from this description. This principle says that a given, static-equilibrium state is stable, if and only if the potential energy is a minimum. We shall not give the complete mathematical expression for this principle in the general case, but confine ourselves to the class of situations whose stability we wish to investigate. We shall confine our interest to instabilities that are excited by perturbations of the equilibrium state that lie wholly "within the plasma"; that is, the initial perturbation vanishes on the plasma's boundaries. More specifically, we assume that the initial perturbations are such that they vanish outside a finite region whose boundaries lie wholly within the plasma. It is clear that in an unbounded medium all instabilities will be of this type. Hereafter, it is to be understood that "instability" means an instability of this type.

For instabilities of the type described, the energy principle can be expressed as follows. A static-equilibrium state is unstable if and only if there exist a perturbation $\underline{\xi}(\underline{r})$ and a volume V, wholly within the plasma, which are such that:

(a) $\underline{\xi}(\underline{r}) = 0$ outside and on the boundary of V and (b) the change in potential energy, δW, of the system caused by this perturbation is negative.

The change in potential energy is given (2) by

$$\delta W = \frac{1}{2}\int_V d\tau\left\{\underline{Q}^2-\underline{j}\cdot(\underline{Q}\times\underline{\xi})+\frac{5}{3}p_\perp(\nabla\cdot\underline{\xi})^2+(\nabla\cdot\underline{\xi})(\underline{\xi}\cdot\nabla p_\perp)+\frac{1}{3}p_\perp(\nabla\cdot\underline{\xi}-3q)^2+q\nabla\cdot(\underline{\xi}(p_{||}-p_\perp)) \right.$$

$$\left.+(p_\perp-p_{||})[(\underline{e}\cdot\nabla\underline{\xi})\cdot(\nabla\underline{\xi}\cdot\underline{e})-(\underline{\xi}\cdot\nabla\underline{e})\cdot(\nabla\underline{\xi}\cdot\underline{e})-4q^2+(\underline{e}\cdot\nabla\underline{\xi})^2-(\underline{\xi}\cdot\nabla\underline{e})\cdot(\underline{e}\cdot\nabla\underline{\xi})]\right\} \quad (1)$$

where

$$\underline{Q} \equiv \nabla\times(\underline{\xi}\times\underline{B}) \quad (2)$$

and

$$q = \underline{e}\cdot(\underline{e}\cdot\nabla\underline{\xi}) \quad (3)$$

In Eqs. 1-3 all quantities take their unperturbed values (except $\underline{\xi}$, of course).

c. Instabilities in a Uniform Plasma

We shall now consider the equilibrium state in which all quantities are constant in space. Introduce a Cartesian coordinate system with x-axis along $\underline{B}$. Introducing the symbols $\alpha \equiv p_\perp/B^2$ and $\beta \equiv p_{||}/B^2$, and using Eq. 1, we obtain

$$\delta W = \frac{1}{2}\int_V d\tau\cdot B^2\left\{(1+\alpha-\beta)\left[\left(\frac{\partial\xi_y}{\partial x}\right)^2+\left(\frac{\partial\xi_z}{\partial x}\right)^2\right]+(1+3\beta)\left(\frac{\partial\xi_x}{\partial x}\right)^2+(1+2\alpha)(\nabla\cdot\underline{\xi})^2\right.$$

$$\left.-2(1+\alpha)\left(\frac{\partial\xi_x}{\partial x}\right)(\nabla\cdot\underline{\xi})+(\alpha-\beta)\left[\left(\frac{\partial\underline{\xi}}{\partial x}\right)\cdot(\nabla\xi_x)-\left(\frac{\partial\xi_x}{\partial x}\right)(\nabla\cdot\underline{\xi})\right]\right\} \quad (4)$$

We can now perform the transformations:

$$(a-\beta)\left[\left(\frac{\partial \underline{\xi}}{\partial x}\right)\cdot(\nabla\xi_x) - \left(\frac{\partial \xi_x}{\partial x}\right)(\nabla\cdot\underline{\xi})\right] = \frac{\partial}{\partial x}\left[(a-\beta)(\underline{\xi}\cdot\nabla\xi_x)\right] - \nabla\cdot\left[(a-\beta)\frac{\partial \xi_x}{\partial x}\,\underline{\xi}\right]$$

$$(1+2a)(\nabla\cdot\underline{\xi})^2 - 2(1+a)\frac{\partial \xi_x}{\partial x}(\nabla\cdot\underline{\xi}) = \frac{1}{1+2a}\left[(1+2a)(\nabla\cdot\underline{\xi}) - (1+a)\left(\frac{\partial \xi_x}{\partial x}\right)\right]^2 - \frac{(1+a)^2}{1+2a}\left(\frac{\partial \xi_x}{\partial x}\right)^2$$

Substitute these transformations in Eq. 4. Then we get

$$\delta W = \frac{1}{2}\int_V d\tau\, B^2\left\{(1+a-\beta)\left[\left(\frac{\partial \xi_y}{\partial x}\right)^2 + \left(\frac{\partial \xi_z}{\partial x}\right)^2\right] + \frac{1}{1+2a}\left[(1+2a)(\nabla\cdot\underline{\xi}) - (1+a)\left(\frac{\partial \xi_x}{\partial x}\right)\right]^2 + \left(3\beta - \frac{a^2}{1+2a}\right)\left(\frac{\partial \xi_x}{\partial x}\right)^2 + \frac{\partial}{\partial x}\left[(a-\beta)(\underline{\xi}\cdot\nabla\xi_x)\right] - \nabla\cdot\left[(a-\beta)\frac{\partial \xi_x}{\partial x}\,\underline{\xi}\right]\right\} \qquad (5)$$

From the boundary conditions for $\underline{\xi}$ on the boundary of V, it follows that the last two terms in the integrand will give no contribution to the integral.

It is now easy to find a sufficient condition for stability. We have

$$\delta W \geq \frac{B^2}{2}\int_V d\tau\left\{(1+a-\beta)\left[\left(\frac{\partial \xi_y}{\partial x}\right)^2 + \left(\frac{\partial \xi_z}{\partial x}\right)^2\right] + \left(3\beta - \frac{a^2}{1+2a}\right)\left(\frac{\partial \xi_x}{\partial x}\right)^2\right\}$$

Introduce $A \equiv 1 + a - \beta$ and $C \equiv 3\beta - (a^2/1+2a)$. It is clear that for all $\underline{\xi}$ and V, $\delta W > 0$, if $A > 0$ and $C > 0$. The curves $A = 0$ and $C = 0$ are drawn in Fig. II-11. We see that

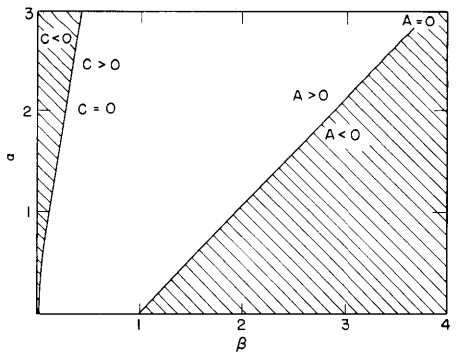

Fig. II-11. Regions of stability (unshaded) and instability (shaded).

$A = 0$ implies $C > 0$, and that $C = 0$ implies $A > 0$. Hence, we can say that $A \geq 0$ and $C \geq 0$ is a sufficient condition for stability.

We shall now show that this condition is also necessary for stability. This is equivalent to showing that $A < 0$ or $C < 0$ is sufficient for instability. Define a function ϕ as

$$\phi(x, y, z) = (1 - \cos mx)(1 - \cos ny)\, f(z)$$

where m and n are integers, $f(z) = 0$ for $z = 0$ and $z = 2\pi$, and is arbitrary otherwise. Choose a perturbation $\underline{\xi}$ which is such that

$$\left.\begin{aligned} \xi_x &= \frac{\partial \phi}{\partial y} \\ \xi_y &= -\gamma \frac{\partial \phi}{\partial x} \\ \xi_z &= 0 \end{aligned}\right\} \text{ inside K} \qquad \underline{\xi} = 0 \text{ outside K}$$

where $\gamma = a/(1+2a)$, and K is a cube with corners in the points: $(2\pi, 0, 0)$, $(0, 2\pi, 0)$, $(0, 0, 2\pi)$, $(2\pi, 2\pi, 0)$, $(2\pi, 0, 2\pi)$, $(0, 2\pi, 2\pi)$, $(2\pi, 2\pi, 2\pi)$, $(0, 0, 0)$. We see that $\underline{\xi}$ is continuous and vanishes on the boundary of K, and that $\underline{\xi}$ is so chosen that

$$(1+2a)\, \nabla \cdot \underline{\xi} - (1+a) \frac{\partial \xi_x}{\partial x} = 0$$

For δW we get

$$\delta W = \frac{B^2}{2} \int_K d\tau \left\{ A \left(\frac{\partial^2 \phi}{\partial x^2} \right)^2 \gamma^2 + C \left(\frac{\partial^2 \phi}{\partial x \partial y} \right)^2 \right\}$$

which yields

$$\delta W = \frac{B^2}{2} \cdot \int_0^{2\pi} f(z)^2 \, dz \cdot (A\gamma^2 3\pi^2 m^2 + C\pi^2 n^2)\, m^2$$

We see that if either condition, $A < 0$ or $C < 0$, is fulfilled, then δW can always be made negative by a suitable choice of m and n.

The net result is, therefore, that the plasma is stable if and only if both A and C are greater than or equal to zero. The regions for stability and instability are shown in Fig. II-11.

d. Comparison with Previous Results

Hydromagnetic instabilities of the type considered in this paper have been mentioned by W. B. Thomson (4). He states that instabilities will occur if $\beta \gg a$ and $\beta > 1/4$. It appears that the second of these conditions is not in conformity with our results. Agreement is reached if the condition $\beta > 1/4$ is replaced by $\beta > 1$. The result given in Thomson's paper is based upon the same energy principle as the one that we have employed. Since the calculations leading to this result are not published, we cannot find the reason for this (slight) lack of agreement.

Rosenbluth (1) has investigated the stability of hydromagnetic waves in a uniform

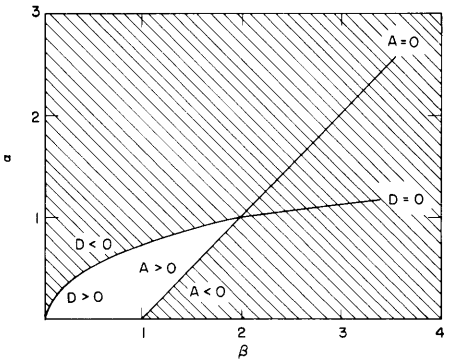

Fig. II-12. Regions of stability (unshaded) and instability (shaded) according to M. N. Rosenbluth.

plasma of the type considered in this report. According to him, a sufficient condition for instability is given by

$$A = 1 + \alpha - \beta < 0 \text{ or } D \equiv \frac{1}{2} - \frac{\alpha^2}{\beta} < 0$$

The curves for A = 0 and D = 0 are drawn in Fig. II-12. The condition A < 0 is identical with our own. The condition D < 0, however, is essentially different from our C < 0.

We note that Rosenbluth's result implies instability — even in the isotropic case. This is surprising. It follows directly from the basic energy variation integral in Eq. 1 that δW is positive for all $\underline{\xi}$ if we set $p_{\parallel} =$ [illegible].

e. Two-Dimensional Generalization

We shall now treat a more general equilibrium state than the uniform one. The magnetic field is assumed to be everywhere parallel to the x-axis, and all equilibrium quantities are assumed to be constant along this axis. The variations perpendicular to the x-axis are arbitrary and subject only to the equilibrium conditions.

The equilibrium condition is

$$-\nabla \cdot \underline{\underline{P}} + \underline{j} \times \underline{B} = 0$$

This can be rewritten

$$\nabla \left(p_{\perp} + \frac{B^2}{2} \right) = 0$$

if we remember that $\frac{\partial}{\partial x}\left(p_{\perp} + \frac{B^2}{2} \right)$ is assumed to be equal to zero. For δW we obtain, from Eq. 1:

$$\delta W = \frac{1}{2}\int_V d\tau \left\{ \underline{Q}^2 - \underline{j}\cdot(\underline{Q}\times\underline{\xi}) + (\nabla\cdot\underline{\xi})(\underline{\xi}\cdot\nabla p_\perp) + \frac{5}{3}p_\perp(\nabla\cdot\underline{\xi})^2 + \frac{1}{3}p_\perp\left(\nabla\cdot\underline{\xi} - 3\frac{\partial\xi_x}{\partial x}\right)^2 \right.$$
$$\left. + (p_\perp - p_\parallel)\left[-4\left(\frac{\partial\xi_x}{\partial x}\right)^2 + \left(\frac{\partial\underline{\xi}}{\partial x}\right)^2\right] + (p_\perp - p_\parallel)\left(\frac{\partial\underline{\xi}}{\partial x}\right)\cdot(\nabla\xi_x) + \frac{\partial\xi_x}{\partial x}\nabla\cdot[\underline{\xi}(p_\parallel - p_\perp)] \right\} \tag{7}$$

Now it can be seen that

$$(p_\perp - p_\parallel)\left(\frac{\partial\underline{\xi}}{\partial x}\right)\cdot(\nabla\xi_x) - \frac{\partial\xi_x}{\partial x}\nabla\cdot[\underline{\xi}(p_\perp - p_\parallel)] = \frac{\partial}{\partial x}[(p_\perp - p_\parallel)(\underline{\xi}\cdot\nabla\xi_x)] - \nabla\cdot\left[(p_\perp - p_\parallel)\frac{\partial\xi_x}{\partial x}\underline{\xi}\right] \tag{8}$$

For the term $\underline{Q}^2$, we obtain

$$\underline{Q}^2 = B^2\left(\frac{\partial\underline{\xi}}{\partial x}\right)^2 + B^2(\nabla\cdot\underline{\xi})^2 + (\underline{\xi}\cdot\nabla\underline{B})^2 - 2B^2\left(\frac{\partial\xi_x}{\partial x}\right)(\nabla\cdot\underline{\xi}) + \left(\nabla\cdot\underline{\xi} - \frac{\partial\xi_x}{\partial x}\right)(\underline{\xi}\cdot\nabla B^2) \tag{9}$$

The term $-\underline{j}\cdot(\underline{Q}\times\underline{\xi})$ gives

$$-\underline{j}\cdot(\underline{Q}\times\underline{\xi}) = \underline{\xi}\cdot\left(\nabla\frac{B^2}{2}\right)\left(\frac{\partial\xi_x}{\partial x}\right) - \underline{\xi}\cdot\nabla\left(\frac{B^2}{2}\right)(\nabla\cdot\underline{\xi}) - (\underline{\xi}\cdot\nabla\underline{B})^2 - \xi_x\left(\frac{\partial\underline{\xi}}{\partial x}\right)\cdot\left(\nabla\frac{B^2}{2}\right) \tag{10}$$

Substituting Eqs. 8, 9, and 10 in Eq. 7, we get

$$\delta W = \frac{1}{2}\int_V d\tau \left\{ B^2\left(\frac{\partial\underline{\xi}}{\partial x}\right)^2 + B^2(\nabla\cdot\underline{\xi})^2 - 2B^2\left(\frac{\partial\xi_x}{\partial x}\right)(\nabla\cdot\underline{\xi}) + \frac{5}{3}p_\perp(\nabla\cdot\underline{\xi})^2 + \frac{1}{3}p_\perp\left(\nabla\cdot\underline{\xi} - 3\frac{\partial\xi_x}{\partial x}\right)^2 \right.$$
$$\left. + (p_\perp - p_\parallel)\left[-4\left(\frac{\partial\xi_x}{\partial x}\right)^2 + \left(\frac{\partial\underline{\xi}}{\partial x}\right)^2\right] \right\} + \frac{1}{2}\int_V d\tau \left\{ (\nabla\cdot\underline{\xi})\,\underline{\xi}\cdot\nabla\left(p_\perp + \frac{B^2}{2}\right) - \frac{\partial}{\partial x}\left(\xi_x\underline{\xi}\cdot\nabla\frac{B^2}{2}\right) \right.$$
$$\left. + \frac{\partial}{\partial x}[(p_\perp - p_\parallel)(\underline{\xi}\cdot\nabla\xi_x)] - \nabla\cdot\left[(p_\perp - p_\parallel)\frac{\partial\xi_x}{\partial x}\cdot\underline{\xi}\right] \right\} \tag{11}$$

From the equilibrium condition and the assumption that $\underline{\xi}$ is equal to zero on the boundary of V, it follows that the last integral in Eq. 11 is equal to zero. It is easy to see that the other integral is identical with the integral in Eq. 5. Hence, by employing the same technique as that used in the uniform case, essentially the same stability conditions will be obtained. However, there is a difference in the two cases, due to the fact that α, β, and B^2 no longer will be constants. It will be realized from the treatment of the uniform case that the size of the volume V is unimportant and can be chosen arbitrarily. Hence we can choose it to be so small that the variations of α, β, and B^2 become unimportant in the integral.

The stability condition can be formulated: The equilibrium state is stable in a certain region if and only if $A \geq 0$ and $C \geq 0$ in all points in the region.

K-F. Voyenli

References

1. M. N. Rosenbluth and others, Proc. Second U. N. Internat. Conf. on the Peaceful Uses of Atomic Energy, Vol. 31, p. 144 (1958).

2. I. Bernstein and others, Proc. Roy. Soc. (London) A 244, 17 (1958).

3. G. F. Chew, M. L. Goldberger, and F. E. Low, Proc. Roy. Soc. (London) A 236, 112 (1956).

4. W. B. Thomson, Proc. Fourth Internat. Conf. on Ionization Phenomena in Gases, p. 555 (1960).

5. PLASMAS IN TRANSVERSE MAGNETIC FIELDS

This report is a continuation of a previous report (1) on an investigation of steady-state configurations of plasmas in a plane transverse to the magnetic field in which they

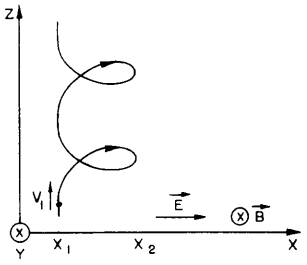

Fig. II-13. Summarizing the geometry of the problem.

are immersed. The plasma is assumed to be collisionless and uniform in the y- and z-directions (see Fig. II-13). The electric and magnetic fields are static, unidirectional, and mutually perpendicular, and are allowed to vary in the x-direction only.

$$\vec{E} = \vec{i}_x E(x) = -\vec{i}_x \frac{d\phi}{dx} \tag{1}$$

$$\vec{B} = \vec{i}_y B(x) = -\vec{i}_y \frac{dA}{dx} \tag{2}$$

The electric and magnetic potentials defined in these equations are subject to the requirements:

$$\frac{d^2\phi}{dx^2} = -\frac{q}{\epsilon_o}[n_i(x)-n_e(x)] \tag{3}$$

$$\frac{dA^2}{dx^2} = -\mu_o q[\Gamma_i(x)-\Gamma_e(x)] \tag{4}$$

where n is the particle density, and Γ is the magnitude of the flux-density vector $\vec{i}_z\Gamma$.

A slight modification is introduced here, in that n and Γ are expressed in terms of the perigee distribution in phase space $f_1(x_1, v_1)$. The quantity $f_1 dx_1 dv_1$ represents the number of particles per unit depth (y) per unit length (z) that have perigees in the range (x_1, dx_1) and perigee velocities in the range (v_1, dv_1).

In order to formulate n and Γ, we need expressions for the velocity components of each particle. These are obtained from the equation of conservation of energy,

$$q\phi(x) + \frac{1}{2}mv_x^2 + \frac{1}{2}mv_z^2 = q\phi(x_1) + \frac{1}{2}mv_1^2 = u \tag{5}$$

and from the conservation of the z component of the canonical momentum,

$$qA(x) + mv_z = qA(x_1) + mv_1 = p \tag{6}$$

Time has been eliminated by setting

$$dt = \frac{dx}{v_x} \tag{7}$$

in accordance with the assumptions stated above. The velocity components of a particle are then available in terms of its instantaneous position x, its perigee position x_1, and its perigee velocity v_1. These expressions are used to define the gyration period,

$$\tau(x_1, v_1) = \frac{2}{\tau}\int_{x_1}^{g_2} \frac{1}{|v_x(x, x_1, v_1)|}\, dx \tag{8}$$

the guiding-center position,

$$x_g(x_1, v_1) = \frac{2}{\tau}\int_{x_1}^{g_2} \frac{x}{|v_x(x, x_1, v_1)|}\, dx \tag{9}$$

and the guiding-center velocity,

$$v_g(x_1, v_1) = \frac{2}{\tau}\int_{x_1}^{g_2} \frac{v_z(x, x_1, v_1)}{|v_x(x, x_1, v_1)|}\, dx \tag{10}$$

where $g_2(x_1, v_1)$ is the apogee of a particle whose perigee is at x_1 and whose perigee velocity is v_1.

Finally, recognizing that each particle will spend a fraction $\frac{2dx}{\tau|v_x|}$ of its time in the range (x, dx), we can formulate n and Γ as

$$n(x) = 2\int_{-\infty}^{\infty} dv_1 \int_{g_1}^{x} \frac{f_1(x_1, v_1)}{\tau(x_1, v_1)} \frac{1}{|v_x(x, x_1, v_1)|}\, dx_1 \tag{11}$$

$$\Gamma(x) = 2\int_{-\infty}^{\infty} dv_1 \int_{g_1}^{x} \frac{f_1(x_1, v_1)}{\tau(x_1, v_1)} \frac{v_z(x, x_1, v_1)}{|v_x(x, x_1, v_1)|} dx_1 \tag{12}$$

where $g_1(x, v_1)$ is the perigee of the particle whose apogee is at x and whose perigee velocity is v_1. The limits on the x_1 integration in the last two equations represent the range of perigees of the particles that can reach x.

If v_1 can be related to x_1, we eliminate it from these equations and replace $f_1(x_1, v_1)$ by the perigee density distribution $n_1(x_1)$.

a. The Perigee Distribution in Phase Space (PPD) and the Boltzmann Distribution Function

The PPD was introduced in order to permit the formulation of the problem in terms of the results of an exact trajectory analysis. We need to relate it to the Boltzmann distribution function, $f(x, v_x, v_z)$. To accomplish this, we construct the function $f'(x, v_x, v_z, x_1, v_1)$, which tells us how many particles in the phase-volume element $[(x, dx), (v_x, dv_x), (v_z, dv_z)]$ have perigees within $[(x_1, dx_1), (v_1, dv_1)]$. The five variables involved in f' are ostensibly independent. However, f' must vanish unless these variables satisfy the equations of motion, Eqs. 5 and 6. We therefore construct f' from the integrand of Eq. 11 combined with Eqs. 5 and 6:

$$f' = \frac{f_1(x_1, v_1)}{\tau(x_1, v_1)} \frac{1}{v_x} u_o\left\{v_x - \left(\frac{2}{m}\right)^{1/2}\left[u(x_1, v_1) - q\phi(x) - \frac{1}{2}mv_z^2\right]^{1/2}\right\} u_o\left\{v_x - \frac{1}{m}[p(x_1, v_1) - qA(x)]\right\} \tag{13}$$

where u_o is the impulse (or Dirac delta) function. Omitting the details of the integration, we obtain the Boltzmann distribution function

$$f(x, v_x, v_z) = 2\frac{f_1(\alpha, \beta)}{\tau(\alpha, \beta)} \frac{1}{(q/m)[E(\alpha) - \beta B(\alpha)]} \tag{14}$$

where α and β are the perigee position and velocity of the particle that has the velocity components v_x and v_z at x, and satisfy the equations

$$q\phi(\alpha) + \frac{1}{2}m\beta^2 = q\phi(x) + \frac{1}{2}mv_x^2 + \frac{1}{2}mv_z^2 = u \tag{15}$$

$$qA(\alpha) + m\beta = qA(x) + mv_z = p \tag{16}$$

Note that f' is indeed expressible in terms of the constants of the motion, u and p. Note also that $(q/m)[E(\alpha) - \beta B(\alpha)]$ is the perigee acceleration of the particle.

b. Transport Equations

Having established the connection between the PPD and the Boltzmann distribution function, we are assured that the transport equations can be constructed from it. The conservation of mass is trivially satisfied. The conservation of momentum can be obtained by defining the pressure-tensor component

$$P_{xx} = \overline{nmv_x^2} = 2m \int_{-\infty}^{\infty} dv_1 \int_{g_1}^{x} \frac{f_1}{\tau} |v_x| \, dx_1 \tag{17}$$

and differentiating it with respect to x. Since v_x vanishes at both limits, we need only evaluate the integral of $\frac{f_1}{\tau} \frac{\partial v_x}{\partial x}$. The derivative $\partial v_x/\partial x$ is evaluated from Eqs. 5 and 6 and substituted in the integral. Comparison of the form of the resultant integral with Eqs. 11 and 12 leads to the familiar equation

$$0 = -\frac{dP_{xx}}{dx} + qn(x)\, E(x) - q\Gamma(x)\, B(x) \tag{18}$$

c. Guiding-Center Velocity and Flow Velocity

The derivation of Eq. 18 is not surprising (the macroscopic variables "do not know" the distribution function from which they were obtained). It does, however, emphasize the fact that the results of orbit theory and transport theory must agree, despite the fact that the guiding-center velocity, v_g, generally differs from the flow velocity, $v_f = \Gamma/n$. We might mention the case of the uniform plasma immersed in a transversely varying magnetic field; here, the difference is acute $\left(v_g \propto \vec{B} \times \text{grad } B^2, v_f = 0\right)$, but it has been reconciled by Spitzer (2) and Tonks (3) in the limit of small orbits. To this we might add the case presented in our previous report (1), in which a uniform electron plasma is immersed in a uniform magnetic field and supports a linearly varying electric field. In this case, $\vec{v}_g = \vec{E} \times \vec{B}/B^2$, whereas Eq. 12 predicts no flow.

To establish the connection between the two velocities, consider a filament of particles with perigees in the range (x_1, dx_1) and perigee velocities in the range (v_1, dv_1). The contribution of these particles to the total flux across any plane, z = constant, can be computed in two ways. On the one hand, we can assign each particle a guiding-center velocity v_g, and express this contribution as

$$\delta I = dx_1 dv_1 f_1(x_1, v_1)\, v_g(x_1, v_1) \tag{19}$$

On the other hand, we can consider the contribution of these particles to the flux density given by Eq. 12:

$$\delta\Gamma(x) = 2dx_1 dv_1 \frac{f_1}{\tau}\frac{v_z}{|v_x|} \tag{20}$$

This expression is valid only in the range $g_2(x_1, v_1) \geq x \geq x_1$; the flux density vanishes outside this range. The total flux of these particles is, then,

$$\delta I = \int_{x_1}^{g_2} \delta\Gamma(x)\, dx = dx_1 dv_1 f_1(x_1, v_1)\frac{2}{\tau}\int_{x_1}^{g_2}\frac{v_z}{|v_x|}dx \tag{21}$$

The expressions given in Eqs. 19 and 20 are identical, by virtue of Eq. 10. We can generalize this result to any finite slab of plasma, concluding that the total flow in such a slab is given correctly by either method of accounting.

In order to apply these results to the specific cases mentioned above, consider the semi-infinite slab of plasma shown in Fig. II-14. In order to terminate the slab, we ask that f_1 shall vanish for $x > b_1$. There will be a boundary layer $b_2 \geq x \geq b_1$, which is established by particles whose perigees lie within two Larmor radii at the left of b_1. In both cases, Eqs. 12 and 18 would predict no net flux density for $x < b_1$, while the equations of motion indicate that each particle has a finite guiding-center velocity v_g. However, the apparent guiding-center flux calculated from v_g really resides in the boundary layer, and is computed correctly by applying Eq. 12 to that layer. Note that this renders the analysis previously reported (1) exact, since the assumption of a uniform magnetic field in the body of the plasma is consistent with the absence of flux in that region.

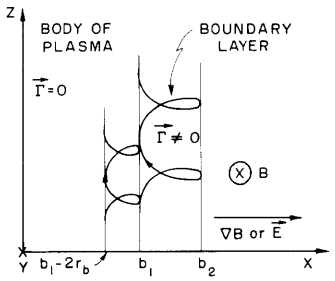

Fig. II-14. Boundary layer at the edge of a plasma slab.

S. Frankenthal

References

1. D. J. Rose and S. Frankenthal, Quarterly Progress Report No. 55, Research Laboratory of Electronics, M. I. T., Oct. 15, 1959, pp. 30-34.

2. L. Spitzer, Jr., Astrophys. J. 116, 299 (1952).

3. L. Tonks, Phys. Rev. 97, 1443 (1955).

II-B. PLASMA ELECTRONICS*

Prof. L. D. Smullin
Prof. H. A. Haus
Prof. A. Bers
Prof. D. J. Rose
P. Chorney
L. J. Donadieu
T. H. Dupree
T. J. Fessenden
W. D. Getty
H. Y. Hsieh
L. M. Lidsky
D. L. Morse
A. Peskoff
S. D. Rothleder
M. C. Vanwormhoudt
R. C. Wingerson
S. Yoshikawa

RESEARCH OBJECTIVES

1. Plasmas for Electrical Energy Conversion

During the coming year the work of this group will be concerned with the following problems:

Interaction between an Electron Beam and a Plasma. Theoretical and experimental studies are being made of the levels of oscillation that can be induced in a plasma by a high-speed electron beam. Present experiments are based on the hollow-cathode arc and a 10-kev, 1-amp electron beam. Other experiments, with the use of two beams, or of a reflected electron beam, are now being planned.

Hollow-Cathode Arc. The hollow-cathode arc has turned out to be an extremely interesting device. We plan to make detailed parametric studies of its characteristics. The effects of arc length, magnetic-field strength, and thermal properties of the cathode on electron density, temperature, and diffusion will be studied.

Reflex (Penning Ionization Gauge) Discharges. Noise and diffusion properties of reflex discharges are being studied. Our principle interest is in determining what factors govern the limiting charge density in such discharges.

High-Power Microwave Discharges. Studies have been made of the maximum electron density attainable in a high-power, microwave discharge, with no dc magnetic field. With pressures of approximately 1 mm Hg, electron densities of 10^{13}-10^{14}/cc can be achieved. In the coming period, the use of a superimposed dc magnetic field will be studied. This will allow much more power to be coupled into the plasma if $\omega \approx \omega_c$, and thus a larger percentage of ionization will be attainable.

Millimeter-Wave Diagnostic Tools for Plasmas. A 2-mm (150 kmc) system for studying plasmas is being designed. Lenses and horns for producing collimated and focused beams are being designed.

Magnetohydrodynamic Power Generation. A theoretical study will be made of the possibility of generating power through the interaction of traveling waves with fast streams of conducting gases. Such schemes provide certain advantages over dc magnetohydrodynamic generators, such as the absence of current flow from gas to wall, and direct generation of ac power.

Thermal Noise in Plasmas. The theoretical work already reported on thermal noise in uniform dissipative media will be extended to nonuniform media. Application to the study of noise in plasma sheets will be sought.

Plasma Waveguides. Theoretical work on uniform plasma waveguides will continue.

L. D. Smullin, H. A. Haus, A. Bers

*This work was supported in part by National Science Foundation under Grant G-9330.

(II. PLASMA DYNAMICS)

2. Plasmas for Nuclear Energy Conversion

This group is concerned with the eventual conversion of nuclear energy to useful purposes with the use of plasmas. Our principal activity is research in plasma physics and related fields that are basic to any future development of controlled fusion. This work is divided into studies of plasma kinetic theory, related particularly to plasma thermalization, energy transfer, and stability; experimental study of small highly ionized plasmas; plasma acceleration, both for plasma injection in possible fusion devices and for space propulsion; and the engineering developments necessary for large plasma devices such as superconducting magnet systems. Another activity is related to the application of cesium plasma diodes to direct conversion of heat from hot fission reactors to electricity.

D. J. Rose

1. THERMAL NOISE FROM PLASMAS

In order to account for the noise properties of lossy networks in thermodynamic equilibrium, it is customary to introduce noise sources that are associated with the resistors of the network. This amounts to writing Kirchhoff's equations with random driving terms. The properties of these sources are then derived from Nyquist's noise theorem. A similar procedure is used in this study to account for the noise generated by linear lossy electromagnetic media (1). A random current-density driving term is added to Maxwell's equations. An extension of Nyquist's reasoning allows us to determine the statistical properties of these noise currents. The only restriction imposed upon the type of medium that can be handled in this way is that is must be linear and time-invariant. This means that the current density in the medium will be given by a relation of the form (column matrices represent vectors):

$$\mathbf{J}(\bar{r}, t) = \int_{-\infty}^{\infty} d\alpha \int_{C} d\tau_s \, \mathbf{g}(\bar{r} \,|\, \bar{s}, t-\alpha) \, \mathbf{E}(\bar{s}, \alpha)$$

or in the sinusoidal steady state at frequency f:

$$\mathbf{J}(\bar{r}, f) = \int_{C} d\tau_s \, \mathbf{G}(\bar{r} \,|\, \bar{s}, f) \, \mathbf{E}(\bar{s}, f)$$

Here, g and G are dyadic Green's operators and are the Fourier transforms of each other, and C is the volume covered by the lossy material.

The relation that is obtained from Nyquist's argument is that the crosscorrelation matrix of the random driving-current sources $\mathbf{J}(\bar{r}, t)$ is given by

$$\phi(\bar{r} \,|\, \bar{s}, \tau) = \lim_{T \to \infty} \frac{1}{2T} \int_{-T}^{T} dt \, \mathbf{J}(\bar{r}, t+\tau) \, \mathbf{J}(\bar{s}, t)$$

$$= kT[\mathbf{g}(\bar{r} \,|\, \bar{s}, \tau) + \mathbf{g}(\bar{s} \,|\, \bar{r}, -\tau)]$$

The cross-power density matrix is likewise given by

$$\phi(\bar{r}\,|\,\bar{s}, f) = kT[G(\bar{r}\,|\,\bar{s}, f)+G^{+}(\bar{s}\,|\,\bar{r}, f)]$$

These results state, then, that at thermodynamic equilibrium, the noise-current correlation matrix is proportional to the loss matrix of the medium, the proportionality constant being given by kT (k is Boltzmann's constant, T is the absolute temperature). Since $\phi(\bar{r}\,|\,\bar{s}, f)$ is a positive semidefinite operator, in the sense that

$$\int_C \int_C d\tau_r d\tau_s \; u^{+}(\bar{r})\; \phi(\bar{r}\,|\,\bar{s}, f)\; u(\bar{s}) \geq 0$$

we find that the noise generated in a medium can only be accounted for by a source term in Maxwell's equations if the loss of the medium is also positive semidefinite. This is obviously the case for passive media.

Onsager's reciprocity relations can be formulated in a very general way: $\phi(\bar{r}\,|\,\bar{s}, \tau)$ must be even in τ or $\phi(\bar{r}\,|\,\bar{s}, f)$ must be pure real. This is known as the condition for microscopic reversibility.

The formalism was applied to a one-dimensional, collision-free plasma (Landau assumptions) under small-signal conditions. This is a medium in which current and electric field are related by a set of linear integrodifferential equations. The inhomogeneous case was treated by finding $g(\bar{r}\,|\,\bar{s}, \tau)$ by the method of characteristics. Expressions were found for $\phi(\bar{r}\,|\,\bar{s}, \tau)$ and $\phi(\bar{r}\,|\,\bar{s}, f)$ in terms of integrals pertaining to the unperturbed electron motions. We found that the conditions for microscopic reversibility and for positive semidefiniteness of the Landau loss were met.

Three simpler cases that yield a better insight into the physical aspects of the problem have been treated: (a) an unbounded homogeneous plasma; (b) a homogeneous plasma of infinite extent but bounded by an impenetrable wall; and (c) a homogeneous plasma bounded by two parallel impenetrable walls. In case (c) the losses are due solely to electrons that travel back and forth between the walls in a time that is equal to an exact multiple of the rf period.

These three cases have also been treated by direct integration of the Boltzmann equation. The results are identical with those of the previous method, but only if, in some improper integrals, the frequency variable p approaches the $j\omega$-axis from the right. This reflects the fact that in all physical situations, we start with an unexcited plasma; p is thus used as a Laplace transform variable. It is only under this condition that the computed loss (with no collision term in the basic equations) will represent the limit toward which the losses of an actual plasma will tend if collisions become very infrequent. The Green's-function approach does not involve these fine points about limits

of improper integrals, because the fact that we start with an unexcited plasma is built into the causality condition $g(\bar{r}\,|\,\bar{s}, \tau) = 0$ for all $\tau < 0$.

M. C. Vanwormhoudt

References

1. H. A. Haus, Thermal noise from plasmas, Quarterly Progress Report No. 59, Research Laboratory of Electronics, M. I. T., Oct. 15, 1960, pp. 15-21.

2. MICROWAVE DIAGNOSTICS OF THE HOLLOW-CATHODE-DISCHARGE PLASMA

The object of our preliminary microwave diagnostic experiment was to determine the approximate electron density in the center of the plasma column of the hollow-cathode discharge. In our most recent experiments, we used essentially the same microwave reflection method described in Quarterly Progress Report No. 58, pages 35-41, except that the microwave oscillator frequency was fixed at 36 kmc and the variation of power reflected from the plasma was observed as a function of discharge current instead of oscillator frequency. The reflected power was determined by measuring the dc component of current through a crystal mounted on the directional coupler (1). An example of our measurements is shown in Fig. II-15 for the given discharge parameters. In the arc current range (20-40 amp) the plasma changes from a transparent to an opaque medium; this indicates that the effective electron density for this particular curve is of the order of 10^{13} electrons/cc. A density measurement made with a Langmuir probe placed near the edge of the visible discharge column yields the same order of magnitude with the discharge current set at 20 amp. We conclude, therefore, that for the given operating conditions, the plasma has an average density in the range 10^{13}-10^{14} electrons/cc.

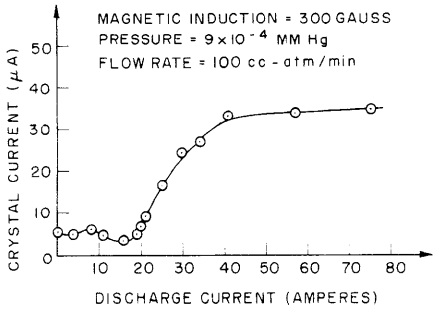

Fig. II-15. Experimental curve of crystal current proportional to reflected power as a function of discharge current.

We have found that curves similar to the curve of Fig. II-15 could be obtained over a narrow range of pressure and gas-flow rate with the oscillator frequency fixed at 36 kmc. The effect of higher magnetic induction is to shift the transition from transparency to opacity toward lower discharge currents.

Further information about the plasma can be obtained from a simple analysis of this

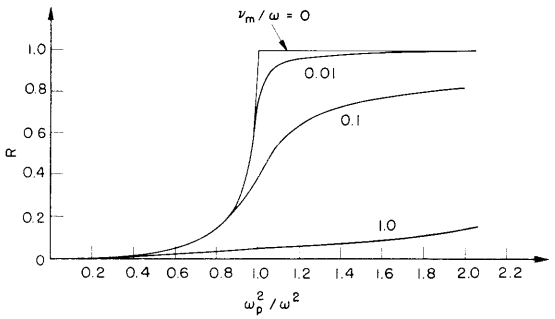

Fig. II-16. Fraction of incident power reflected from a semi-infinite plasma for various values of ν_m/ω.

experiment. The general shape of the reflected power curve suggests that the semi-infinite, uniform plasma is a reasonable model of the plasma produced by the discharge. Since the cyclotron frequency is negligible in comparison with the plasma resonant frequency, the relative dielectric constant of the plasma is

$$K = 1 - a^2 \frac{1}{1 - j(\nu_m/\omega)}$$

where $a = \omega_p/\omega$ and ν_m is the electron collision frequency. The ratio of reflected to incident power for an incident TEM wave is

$$R = \left| \frac{1 - \sqrt{K}}{1 + \sqrt{K}} \right|^2$$

This equation is plotted in Fig. II-16 for various values of ν_m/ω, the ratio of the collision frequency for momentum transfer to the frequency of the externally applied field. If we assume that the electron density is proportional to the discharge current, the coordinates of our experimental curve differ from the coordinates of Fig. II-16 by constant factors. Using these two constants to normalize the coordinates of our experimental curve, we obtain an approximate fit to the theoretical curve for $\nu_m/\omega = 0.1$ in Fig. II-16, and as a result we obtain $\nu_m = 2.3 \times 10^{10}$ sec^{-1}. If we assume an electron temperature of 3 ev, which is a reasonable assumption based on the results of our work with Langmuir probes, and use a collision probability, taken from Brown (2), for electrons in argon of 25 collisions/cm, we find that the pressure required for the suggested ν_m is approximately 7 mm Hg, compared with 10^{-3} mm Hg at the gauge. The existence of this pressure difference is unlikely in the arc vacuum system, even if we consider the effect of the jet of gas emerging from the hollow cathode. The frequency of collisions between electrons and ions has also been calculated by using the formula given by Spitzer (3). Assuming that the charged-particle density is 2×10^{13} particles/cm^3, we find that the

electron-ion collision frequency is 2×10^8 sec^{-1}, or $\nu_m/\omega = 0.001$. Electron collisions, therefore, are not solely responsible for the rounding of our experimental curve. In order to obtain more detailed information about the discharge plasma from this experiment, it will be necessary to investigate the effects of electron-density gradients and the radiation pattern of the waveguide on the reflection coefficient. In addition, we must determine whether or not the assumption that discharge current is proportional to electron density is valid.

W. D. Getty

References

1. W. D. Getty and L. D. Smullin, Experimental results of the study of the hollow-cathode discharge, Quarterly Progress Report No. 58, Research Laboratory of Electronics, M. I. T., July 15, 1960, pp. 35-41.

2. S. C. Brown, Basic Data of Plasma Physics (Technology Press of Massachusetts Institute of Technology, Cambridge, Mass., 1959), see Chapter 1.

3. L. Spitzer, Jr., Physics of Fully Ionized Gases (Interscience Publishers, Inc., New York, 1956), see Chapter 5.

3. MEASUREMENT OF A DENSE PLASMA IN A RESONANT CAVITY

The usual method of determining the electron density and collision frequency of a plasma in a resonant cavity is through the measurement of the perturbing effects of the plasma on an empty-cavity mode. This method is limited to the measurement of electron densities less than, or at most, slightly greater than that which produces plasma resonance ($\omega = \omega_p$). In this report a perturbation technique is developed that utilizes the perturbation of a cavity mode which would exist if the plasma were replaced by a perfect conductor. This method is valid only when the plasma frequency is much greater than the applied frequency and, therefore, is useful for measuring a dense plasma that partially fills a resonant cavity.

Everhart (1) has shown that the ac conductivity of a plasma is given by

$$\sigma = \left(\frac{\omega_p}{\omega}\right)^2 \frac{\omega\epsilon_o}{j + (\nu_c/\omega)} \tag{1}$$

where ω_p is the plasma frequency; ν_c is the electron collision frequency for momentum transfer; and ω is the applied frequency. This equation assumes ν_c to be independent of electron energy. The permittivity and permeability are those of free space (ϵ_o and μ_o).

The intrinsic impedance and propagation constants of a uniform plasma medium can be found from Maxwell's equations and from Eq. 1:

$$Z_p = \left(\frac{j\omega\mu_o}{\sigma + j\omega_o}\right)^{1/2} \approx j\frac{\omega}{\omega_p}\left(\frac{\mu_o}{\epsilon_o}\right)^{1/2}\left(1 - j\frac{\nu_c}{\omega}\right)^{1/2} \tag{2}$$

and

$$\Gamma = \left[j\omega\mu_o(\sigma+j\omega\epsilon_o)\right]^{1/2} \approx \frac{\omega_p}{c}\frac{1}{\left[1-j(\nu_c/\omega)\right]^{1/2}} \tag{3}$$

where c is the velocity of light. The approximations in Eqs. 2 and 3 are valid when ω_p is much greater than ω. The electrical skin depth δ is obtained from Eq. 3.

$$\delta = \frac{1}{\mathrm{Re}\Gamma} = \frac{c}{\omega_p}\frac{\left[1+(\nu_c/\omega)^2\right]^{1/2}}{\mathrm{Re}\left[1+j(\nu_c/\omega)\right]^{1/2}} \tag{4}$$

Notice that both Z_p and δ approach zero as ω_p becomes infinite and the plasma appears as a perfect conductor. This suggests treating the effects of a dense plasma on the properties of a resonant cavity in the same manner as the effects of good, but not perfect, wall conductors are treated.

The shift of the resonant frequency of the cavity and the change in Q caused by a perturbation are obtained from Slater's (2) perturbation formula for cavities. The pertinent relations are

$$\frac{\delta\omega}{\omega} = \frac{\omega - \omega_o}{\omega} = -\frac{\mathrm{Im}\oint_p \vec{E}\times\vec{H}_o^* \cdot d\vec{a}}{2\omega\int_\tau \mu\vec{H}\cdot\vec{H}_o^*\, d\tau} \tag{5}$$

and

$$\frac{1}{Q} - \frac{1}{Q_o} = \frac{\mathrm{Re}\oint_P \vec{E}\times\vec{H}_o^* \cdot d\vec{a}}{\omega\int_\tau \mu\vec{H}\cdot\vec{H}_o^*\, d\tau} \tag{6}$$

The zero subscripts refer to unperturbed quantities. The surface integrals in the numerators of Eqs. 5 and 6 are to be evaluated over the surface of the perturbation, while the integrals in the denominators are to be evaluated over the cavity volume.

These equations can be applied to a dense plasma in a resonant cavity in the following manner. The cavity is assumed to be unperturbed when the volume occupied by the plasma is replaced by a perfect conductor, in which case the quantities $\vec{H}_o$, ω_o, and Q_o are assumed to be known. The perturbed fields $\vec{E}$ and $\vec{H}$ can be expressed approximately

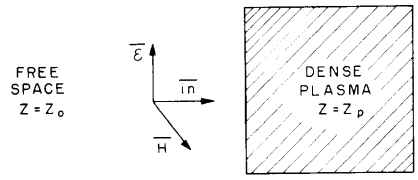

Fig. II-17. Model showing the orientation of a uniform plane wave normally incident on a semi-infinite plasma.

in terms of the unperturbed fields by considering plane wave reflection from a semi-infinite uniform plasma (see Fig. II-17). The fields that exist at the surface of the plasma are found by matching boundary conditions at this surface. We obtain

$$\vec{E} = \frac{-Z_p \vec{i}_n \times \vec{H}_o}{1 + (Z_p/Z_o)} \tag{7}$$

$$\vec{H} = \frac{\vec{H}_o}{1 + (Z_p/Z_o)} \tag{8}$$

where $\vec{H}_o$ is the magnetic field that would exist at the surface if the plasma were replaced by a perfect conductor, and $Z_o = (\mu_o/\epsilon_o)^{1/2}$ is the intrinsic impedance of the medium to the left. If ω_p is much greater than ω, these equations can be simplified to

$$\vec{E} = -Z_p \vec{i}_n \times \vec{H}_o \tag{9}$$

$$\vec{H} = \vec{H}_o \tag{10}$$

Equations 9 and 10 can be used for calculating the perturbation caused by a finite dense plasma in a cavity if the electrical skin depth δ of the plasma is much less than any plasma dimension. The substitution of Eqs. 9, 10, and 2 in Eqs. 5 and 6 yields

$$\frac{\delta\omega}{\omega} = -\frac{c}{2\omega_p} \mathrm{Re}\left(1 - j\frac{\nu_c}{\omega}\right)^{1/2} \mathrm{Kg} \tag{11}$$

and

$$\frac{1}{Q} - \frac{1}{Q_o} = -\frac{c}{\omega_p} \mathrm{Im}\left(1 - j\frac{\nu_c}{\omega}\right)^{1/2} \mathrm{Kg} \tag{12}$$

where Kg is a geometrical constant given by

$$Kg = \frac{\oint_P |\overline{H}_o|^2 \, da}{\int_\tau |\overline{H}_o|^2 \, d\tau} \tag{13}$$

Thus a measurement of the cavity frequency shift and the change in cavity Q caused by the dense plasma will determine both ω_p and ν_c.

T. J. Fessenden

References

1. E. Everhart, Phys Rev. 76, 839 (1949).

2. J. C. Slater, Microwave Electronics (D. Van Nostrand Company, Inc., Princeton, N. J., 1950), p. 67.

4. POWER, ENERGY, GROUP VELOCITY, AND PHASE VELOCITY IN BIDIRECTIONAL WAVEGUIDES

a. Introduction

Some general properties of a broad class of lossless, passive, uniform waveguides are being investigated. This class we refer to as "bidirectional." We define a waveguide mode, which propagates as $\exp(-\Gamma z)$, as bidirectional if it is possible to excite another wave of basically the same field structure that propagates as $\exp(+\Gamma z)$. The z-direction is along the waveguide axis, and Γ is the complex propagation constant.

Waveguides that come under this classification are: (a) those containing isotropic materials; and (b) those containing gyrotropic anisotropic materials with the gyrotropic axis along the waveguide axis. The materials may be inhomogeneous with respect to the waveguide cross section; however, for a given transverse coordinate the materials are axially invariant. A general feature of the materials under consideration is that we allow them to be dispersive; that is, their permittivities and permeabilities may be frequency-dependent. Ferrites and plasmas are prominent examples of dispersive media.

For dispersive media, care must be exercised in the interpretation of stored electromagnetic energy (1-4). It turns out that the so-called energy terms that appear in the complex form of Poynting's theorem do not really represent the time-average energy storage in dispersive media. To distinguish between the actual energy and the energylike terms in Poynting's theorem, we shall refer to the latter as "pseudo energy." The pseudo energy is the same as the actual energy in nondispersive media.

b. Energy, Power, and Group Velocity

The group velocity of a propagating mode is found from an energy theorem (5) which, for lossless, passive, uniform waveguides containing dispersive media, can be shown to be

$$\frac{\partial}{\partial z}\int_A \left[\underline{\bar{E}}_T^* \times \frac{\partial \underline{\bar{H}}_T}{\partial \omega} + \frac{\partial \underline{\bar{E}}_T}{\partial \omega} \times \underline{\bar{H}}_T^*\right] \cdot \bar{i}_z \, da = -j \int_A \left[\underline{\bar{E}}^* \cdot \underline{\underline{\epsilon}}_\omega \cdot \underline{\bar{E}} + \underline{\bar{H}}^* \cdot \underline{\underline{\mu}}_\omega \cdot \underline{\bar{H}}\right] da \tag{1}$$

where the subscript T denotes a field component transverse to the z-direction. The integral expressions, with the integrations carried out over an entire cross section of waveguide, depend only upon the z-coordinate. The quantities $\underline{\underline{\epsilon}}_\omega$ and $\underline{\underline{\mu}}_\omega$ are forms of the permittivity and permeability that give the true energy from the fields, and they are given by

$$\underline{\underline{\epsilon}}_\omega = \frac{\partial}{\partial \omega}\left[\omega \underline{\underline{\epsilon}}\right] \tag{2}$$

$$\underline{\underline{\mu}}_\omega = \frac{\partial}{\partial \omega}\left[\omega \underline{\underline{\mu}}\right] \tag{3}$$

We note that for nondispersive media, $\underline{\underline{\epsilon}}_\omega$ and $\underline{\underline{\mu}}_\omega$ reduce to $\underline{\underline{\epsilon}}$ and $\underline{\underline{\mu}}$, respectively.

We express the fields of a propagating wave by

$$\underline{\bar{E}}(x, y, z) = \underline{\hat{E}}\, e^{-j\beta z} = \left[\underline{\hat{E}}_T + \bar{i}_z \hat{E}_z\right] e^{-j\beta z} \tag{4}$$

$$\underline{\bar{H}}(x, y, z) = \underline{\hat{H}}\, e^{-j\beta z} = \left[\underline{\hat{H}}_T + \bar{i}_z \hat{H}_z\right] e^{-j\beta z} \tag{5}$$

Harmonic time dependence $e^{j\omega t}$ is understood. The circumflex over a field quantity indicates that it has only transverse spatial dependence. When Eqs. 4 and 5 are substituted in Eq. 1, we obtain the reciprocal of the group velocity:

$$\frac{\partial \beta}{\partial \omega} = \frac{W}{P} \tag{6}$$

where

$$W = W_e + W_m \tag{7}$$

$$W_e = \frac{1}{4}\int \underline{\hat{E}}^* \cdot \underline{\underline{\epsilon}}_\omega \cdot \underline{\hat{E}} \, da \tag{8}$$

$$W_m = \frac{1}{4}\int \underline{\hat{H}}^* \cdot \underline{\underline{\mu}}_\omega \cdot \underline{\hat{H}} \, da \tag{9}$$

$$P = \frac{1}{2} \mathrm{Re} \int \underline{\hat{E}}_T \times \underline{\hat{H}}_T^* \cdot \bar{i}_z \, da \tag{10}$$

We interpret P as the time-average power flow in the wave and W as the total time-average energy stored per unit length; W is composed of energy stored in the electric field, in the magnetic field, in the polarization, in the magnetization, and in the kinetic energy of the vibrations of the electric and magnetic dipoles.

Equation 6 applies to all lossless, passive, uniform waveguides, regardless of whether or not they are bidirectional. We confine the following discussion to bidirectional waveguides because of the elegant relations that can be derived for them.

c. Pseudo Energy, Power and Phase Velocity in Bidirectional Waveguides

Waveguides containing materials whose permittivities and permeabilities are of the general form

$$\underline{\underline{\epsilon}} = \begin{bmatrix} \epsilon_1 & -j\epsilon_2 & 0 \\ j\epsilon_2 & \epsilon_1 & 0 \\ 0 & 0 & \epsilon_3 \end{bmatrix} \tag{11}$$

$$\underline{\underline{\mu}} = \begin{bmatrix} \mu_1 & -j\mu_2 & 0 \\ j\mu_2 & \mu_1 & 0 \\ 0 & 0 & \mu_3 \end{bmatrix} \tag{12}$$

can be shown to be bidirectional (6). Expressed mathematically, if a wave of the form

$$\underline{\hat{E}}_+ = [\underline{\hat{E}}_T + \bar{i}_z \underline{\hat{E}}_z] \, e^{-\Gamma z} \tag{13}$$

$$\underline{\hat{H}}_+ = [\underline{\hat{H}}_T + \bar{i}_z \underline{\hat{H}}_z] \, e^{-\Gamma z} \tag{14}$$

can be excited, it is also possible to excite a wave traveling in the opposite direction of the form

$$\underline{\hat{E}}_- = [-\underline{\hat{E}}_T + \bar{i}_z \underline{\hat{E}}_z] \, e^{+\Gamma z} \tag{15}$$

$$\underline{\hat{H}}_- = [+\underline{\hat{H}}_T - \bar{i}_z \underline{\hat{H}}_z] \, e^{+\Gamma z} \tag{16}$$

The subscripts plus and minus denote, respectively, the forward-traveling and backward-traveling waves. Now, if we place a shorting plane across the waveguide cross section at z = 0, it is possible, because of the property of bidirectionality, to set up a standing

wave of the form

$$\underline{\overline{E}}_T = \underline{\hat{E}}_T[e^{-\Gamma z} - e^{+\Gamma z}] \tag{17}$$

$$\underline{\overline{H}}_T = \underline{\hat{H}}_T[e^{-\Gamma z} + e^{+\Gamma z}] \tag{18}$$

$$\underline{E}_z = \underline{\hat{E}}_z[e^{-\Gamma z} + e^{+\Gamma z}] \tag{19}$$

$$\underline{H}_z = \underline{\hat{H}}_z[e^{-\Gamma z} - e^{+\Gamma z}] \tag{20}$$

For lossless, passive, uniform waveguides, the integral form of the Poynting theorem requires that

$$\frac{\partial \underline{P}}{\partial z} = -j2\omega[U_m - U_e] \tag{21}$$

where

$$\underline{P} = \frac{1}{2}\int \underline{\overline{E}}_T \times \underline{\overline{H}}_T^* \cdot \overline{i}_z \, da \tag{22}$$

$$U_m = \frac{1}{4}\int \underline{\overline{H}}^* \cdot \underline{\overline{\mu}} \cdot \underline{\overline{H}} \, da \tag{23}$$

$$U_e = \frac{1}{4}\int \underline{\overline{E}}^* \cdot \underline{\overline{\epsilon}} \cdot \underline{\overline{E}} \, da \tag{24}$$

The time-average complex power flow per waveguide cross section is given by $\underline{P}$. The time-average magnetic pseudo-energy storage per unit length of waveguide is given by U_m, and the time-average electric pseudo-energy storage per unit length is given by U_e. In text books, W is commonly used to denote the stored energy terms in Poynting's theorem. For dispersive media these energylike terms, or pseudo energy, no longer represent the true energy storage. We use the symbol U to denote pseudo energy, and we reserve the symbol W to denote true energy.

When we apply the special form of Poynting's theorem given by Eqs. 21-24 to the fields of the standing wave, Eqs. 17-20, and if we let

$$\Gamma = \alpha + j\beta \tag{25}$$

we obtain the expression

$$[\alpha \cosh 2\alpha z + j\beta \cos 2\beta z]\,\underline{P} = j\omega[(U_m - U_e)\cosh 2\alpha z + (U_T - U_z)\cos 2\beta z] \tag{26}$$

where, now,

$$\underline{P} = \frac{1}{2} \int \underline{\hat{E}}_T \times \underline{\hat{H}}_T^* \cdot \bar{i}_z \, da \tag{27}$$

$$U_m = \frac{1}{4} \int \underline{\hat{H}}^* \cdot \underline{\underline{\mu}} \cdot \underline{\hat{H}} \, da \tag{28}$$

$$U_e = \frac{1}{4} \int \underline{\hat{E}}^* \cdot \underline{\underline{\epsilon}} \cdot \underline{\hat{E}} \, da \tag{29}$$

$$U_T = U_{eT} + U_{mT} \tag{30}$$

$$U_z = U_{ez} + U_{mz} \tag{31}$$

$$U_{eT} = \frac{1}{4} \int \underline{\hat{E}}_T^* \cdot \underline{\underline{\epsilon}}_T \cdot \underline{\hat{E}}_T \, da \tag{32}$$

$$U_{mT} = \frac{1}{4} \int \underline{\hat{H}}_T^* \cdot \underline{\underline{\mu}}_T \cdot \underline{\hat{H}}_T \, da \tag{33}$$

$$U_{ez} = \frac{1}{4} \int \epsilon_3 |\underline{\hat{E}}_z|^2 \, da \tag{34}$$

$$U_{mz} = \frac{1}{4} \int \mu_3 |\underline{\hat{H}}_z|^2 \, da \tag{35}$$

$$\underline{\underline{\epsilon}}_T = \begin{bmatrix} \epsilon_1 & -j\epsilon_2 \\ j\epsilon_2 & \epsilon_1 \end{bmatrix} \tag{36}$$

$$\underline{\underline{\mu}}_T = \begin{bmatrix} \mu_1 & -j\mu_2 \\ j\mu_2 & \mu_1 \end{bmatrix} \tag{37}$$

The quantity U_m is the time-average magnetic pseudo-energy storage per unit length in the incident wave; U_e is the similar electric quantity. The contribution of the transverse fields to the time-average pseudo-energy storage per unit length in the incident wave is given by U_T, and the contribution of the longitudinal fields is given by U_z.

Equation 26 gives us a great deal of novel information that is summarized in Table II-1.

Table II-1. Pseudo energy and power relations in bidirectional waveguide waves.

Propagating Waves	$\Gamma = j\beta$	$\underline{P} = P$	$P = \frac{\omega}{\beta}(U_T - U_z)$	$U_m = U_e$
Cutoff Waves	$\Gamma = \alpha$	$\underline{P} = jQ$	$Q = \frac{\omega}{\alpha}(U_m - U_e)$	$U_T = U_z$
Complex Waves	$\Gamma = \alpha + j\beta$	$\underline{P} = 0$	$U_m = U_e$	$U_T = U_z$

We see from Table II-1 that propagating waves carry pure real power, cutoff waves carry pure reactive power, and complex waves carry no net power at all. Also, we see that in propagating waves, we have an equipartition between electric and magnetic pseudo energy, a result that is well known for nondispersive materials. In cutoff waves, we have an equipartition between transverse and longitudinal pseudo energy. And, in complex waves, we have an equipartition between electric and magnetic pseudo energy, as well as an equipartition between transverse and longitudinal pseudo energy.

d. A Theorem Relating Group and Phase Velocity in Bidirectional Waveguides

The result

$$P = \frac{\omega}{\beta}(U_T - U_z) \tag{38}$$

is most interesting because it is the first time that phase velocity, ω/β, has been related, in general, to the fields of a mode. We may regard this expression as a definition of phase velocity, just as we commonly regard Eq. 6 as a definition of group velocity.

By the elimination of P between Eqs. 6 and 38, we derive the theorem

$$\frac{\partial\beta}{\partial\omega} = \frac{\beta}{\omega}\frac{W}{U_T - U_z} \tag{39}$$

which we shall refer to as the "Bidirectional Waveguide" theorem. We note the general property that group velocity has the sign of the power, since W represents the true energy storage and is hence always positive. Thus, in waves with positive dispersion ($\partial\beta/\partial\omega > 0$), we have $U_T - U_z > 0$; and in waves with negative dispersion ($\partial\beta/\partial\omega < 0$), we have $U_T - U_z < 0$.

Since in propagating waves, $U_m = U_e$, we have two corollaries to this theorem:

$$\frac{\partial\beta}{\partial\omega} = \frac{\beta}{\omega}\frac{W}{2(U_{eT} - U_{mz})} \tag{40}$$

$$\frac{\partial\beta}{\partial\omega} = \frac{\beta}{\omega}\frac{W}{2(U_{mT} - U_{mz})} \tag{41}$$

e. Analogous Expressions for Cutoff Waves

We note in Table II-1 that we have an expression for cutoff waves that is quite similar to Eq. 38, namely

$$Q = \frac{\omega}{a}(U_m - U_e) \tag{42}$$

We may regard Eq. 42 as a definition of the analog of phase velocity in cutoff waves.

An analog of group velocity in cutoff waves can also be found. When the energy theorem, Eq. 1, is applied to the standing wave, Eqs. 17-20, we find that for cutoff waves

$$\frac{\partial a}{\partial \omega} = \frac{(W_{mT} - W_{mz}) - (W_{eT} - W_{ez})}{Q} \tag{43}$$

Combining Eqs. 42 and 43, we have a theorem analogous to Eq. 39.

$$\frac{\partial a}{\partial \omega} = \frac{a}{\omega} \frac{(W_{mT} - W_{mz}) - (W_{eT} - W_{ez})}{U_m - U_e} \tag{44}$$

Since $U_T = U_z$ in cutoff waves, we have the two corollaries:

$$\frac{\partial a}{\partial \omega} = \frac{a}{\omega} \frac{(W_{mT} - W_{mz}) - (W_{eT} - W_{ez})}{2(U_{mT} - U_{ez})} \tag{45}$$

$$\frac{\partial a}{\partial \omega} = \frac{a}{\omega} \frac{(W_{mT} - W_{mz}) - (W_{eT} - W_{ez})}{2(U_{mz} - U_{eT})} \tag{46}$$

f. Illustrative Examples

To illustrate some of the principles developed here, we treat a few illustrative examples that involve inhomogeneous waveguides containing nondispersive, isotropic materials. For such systems there is much simplification because the pseudo energy and the true energy are the same. Thus Eq. 39 becomes

$$\frac{\partial \beta}{\partial \omega} = \frac{\beta}{\omega} \frac{U_T + U_z}{U_T - U_z} \tag{47}$$

Now, $U_T > 0$ and $U_z > 0$; and Adler (7) has shown that $\partial\beta/\partial\omega > 0$ for such systems. Thus we conclude that $U_T > U_z$, and

$$\frac{\partial \beta}{\partial \omega} \geqslant \frac{\beta}{\omega} \tag{48}$$

in lossless waveguides containing nondispersive, isotropic materials. Equation 47 not only proves that phase velocity is greater than or equal to group velocity in these

waveguides but also that $\beta(\omega)$ is monotonically increasing.

As another illustration, we consider the special case in which the waveguide is completely filled by a homogeneous, nondispersive, isotropic material. For this case, in general, we have TE and TM solutions, and for a multiconductor waveguide we have TEM solutions. For the TE modes, a convenient form of Eq. 47 is

$$\frac{\partial\beta}{\partial\omega} = \frac{\beta}{\omega}\frac{U_{eT}}{U_{mT}} \tag{49}$$

and for the TM modes,

$$\frac{\partial\beta}{\partial\omega} = \frac{\beta}{\omega}\frac{U_{mT}}{U_{eT}} \tag{50}$$

For the TEM modes, Eq. 47 simply becomes

$$\frac{\partial\beta}{\partial\omega} = \frac{\beta}{\omega} \tag{51}$$

since $U_z = 0$. Thus we see from Eq. 51 that for TEM waves we have the well-known result that the group and phase velocities are equal, and, furthermore, that β is linear in ω.

For the TE and TM modes, we have

$$Z_o\hat{\underline{E}}_T = \hat{\underline{H}}_T \times \bar{i}_z \tag{52}$$

Here, the characteristic impedance is

$$Z_o = \begin{cases} \dfrac{\omega\mu}{\beta} & \text{for TE modes} \\ \dfrac{\beta}{\omega\epsilon} & \text{for TM modes} \end{cases} \tag{53}$$

Thus

$$U_{eT} = \frac{\epsilon}{\mu}Z_o^2 U_{mT} \tag{54}$$

for both TE and TM modes. The substitution of Eq. 54 in Eq. 49 for TE modes, and in Eq. 50 for TM modes, yields the well-known result

$$\frac{\beta}{\omega}\frac{\partial\beta}{\partial\omega} = \epsilon\mu \tag{55}$$

that is, the product of phase and group velocities is equal to the square of the velocity of light in the medium (8).

It is interesting to note that the solution to the differential equation, Eq. 55, is the dispersion relation

$$\beta^2 = \omega^2 \epsilon \mu + \text{constant} \tag{56}$$

g. Discussion

The novel principles presented here are being studied further, and they are being applied to various sample problems. Special attention is being given to anisotropic systems, such as plasma-loaded waveguides and ferrite waveguides. By means of the Bidirectional Waveguide Theorem, it is hoped that qualitative dispersion properties of these systems can be predicted.

In conclusion, we summarize the new definitions and new physical concepts presented here. First of all, we distinguished between true energy storage and that which we defined as pseudo energy for dispersive media. The discrepancies between these were first recognized by Brillouin (1) who explained that the difference was due to the kinetic energy stored in the motion of the bound charges in dispersive, isotropic dielectrics. A similar explanation holds, of course, for dispersive, anisotropic materials.

We confined our attention to a special class of lossless, passive, uniform waveguides which we defined as bidirectional. For these waveguides — which, incidentally, are not necessarily reciprocal — we derived the novel results presented in Table II-1. It is well known that group velocity can be expressed in terms of the true energy storage and power flow in a propagating wave as in Eq. 6 (1, 4). However, we pointed out that phase velocity can be expressed in terms of pseudo energy and power flow. Another new result for propagating waves is that there is an equipartition of electric pseudo energy and magnetic pseudo energy. Novel, too, are the derived properties of cutoff waves and complex waves. The bidirectional waveguide theorem for propagating waves and the analogous theorem for cutoff waves are derived from the group velocity, expressed in terms of power and energy, and from the phase velocity, expressed in terms of power and pseudo energy.

Only a few of the results in Table II-1 have been previously shown for the special case of nondispersive, isotropic media. Adler (7) has shown that $U_m = U_e$ in propagating waves, that $\underline{P}$ is pure real for propagating waves, and that $\underline{P}$ is pure imaginary in cutoff waves.

Adler has also shown that Γ is either pure real or pure imaginary and is never complex for lossless nondispersive, isotropic media. However, this rule cannot be extended to anisotropic media, and we admit the possibility that complex propagation constants exist when the material is anisotropic. Indeed, complex propagation constants have been calculated by Tai (9) for transversely magnetized lossless ferrite waveguides.

The novel results presented here were derivable because it is possible to set up standing waves in bidirectional waveguides. It is interesting that an examination of a standing wave yields new information about the individual traveling waves that comprise the standing wave.

P. Chorney

References

1. L. Brillouin, Wave Propagation and Group Velocity (Academic Press, Inc., New York and London, 1960).

2. A. Tonning, Energy density in continuous electromagnetic media, Trans. IRE, Vol. AP-8, pp. 428-434, July 1960.

3. T. Hosono and T. Ohira, The electromagnetic energy stored in a dispersive medium, Proc. IRE 48, 247-248 (1960).

4. S. M. Rytov, Some theorems on the group velocity of electromagnetic waves, J. Exptl. Theoret. Phys. (U. S. S. R.) 17, 930-936 (1947).

5. A. Tonning, op. cit., see Section V.

6. A. T. Villeneuve, Orthogonality relationships for waveguides and cavities with inhomogeneous anisotropic media, Trans. IRE, Vol. MTT-7, pp. 441-446, October 1959.

7. R. B. Adler, Properties of Guided Waves in Inhomogeneous Cylindrical Structures, Technical Report 102, Research Laboratory of Electronics, M. I. T., May 27, 1949.

8. See, for instance, J. C. Slater, Microwave Electronics (D. Van Nostrand Co., Inc., New York, 1950), Chapter 3.

9. C. T. Tai, Evanescent modes in a partially filled gyromagnetic rectangular waveguide, J. Appl. Phys. 31, 220-221 (1960).

5. MAGNETOHYDRODYNAMIC AC GENERATOR

Alternating-current generation by converting the directed kinetic energy flow of a hot plasma into electromagnetic power gives promise of two advantages over direct-current generation: the ease of voltage transformation and the possibility of avoiding conduction-current flow between the plasma and the walls of the flow tube.

A study has been started on possible mechanisms of power generation by using plasmas with a time-average velocity. The mechanisms bear close resemblance to power generation and amplification in traveling-wave tubes and klystrons that use electron beams. Simple theoretical models have been constructed, and a linearized analysis of these models has been carried out. They show power gain and indicate the possible use of these principles for ac power amplification and generation.

We study an infinite, parallel-plane, perfectly conducting plasma with a time-average velocity u in the z-direction, a dc magnetic field B_o in the x-direction, and processes with a z-directed ac velocity v, an x-directed B-field, and with z-dependence only. We indicate all time-average quantities except u by the subscript o; all small alternating

quantities are without subscripts.

Force equation: $$\rho_o\left(\frac{\partial v}{\partial t} + u\frac{\partial v}{\partial z}\right) = -\frac{\partial p}{\partial z} - B_o J \tag{1}$$

Maxwell's equation: $$\frac{1}{\mu_o}\frac{\partial B}{\partial z} = J \tag{2}$$

Maxwell's equation: $$-\frac{\partial E}{\partial z} = -\frac{\partial B}{\partial t} \tag{3}$$

Continuity equation: $$\left(\frac{\partial}{\partial t} + u\frac{\partial}{\partial z}\right)\frac{\rho}{\rho_o} = -\frac{\partial v}{\partial z} \tag{4}$$

Ohm's law: $$E = -uB - vB_o \tag{5}$$

Equation of state: $$\frac{p}{p_o} = \gamma\frac{\rho}{\rho_o} \tag{6}$$

Here ρ is the ac mass density, J is the alternating-current density (in the y-direction), E is the ac electric field (in the y-direction). The solutions of these equations under an assumed dependence $\exp[j(\omega t - \beta z)]$ lead to the propagation constants

$$\beta = \frac{\omega}{u \pm c} \tag{7}$$

where

$$c = \left(\gamma\frac{p_o}{\rho_o} + \frac{B_o^2}{\mu_o\rho_o}\right)^{1/2} \tag{8}$$

One wave is fast, with the phase velocity $u_p = u + c$; the other is a slow forward wave, $u_p = u - c$, for $u > c$. For $u < c$, the slow forward wave changes into a wave with negative phase velocity. The group velocity is given by

$$\frac{d\omega}{d\beta} = u \pm c \tag{9}$$

for fast and slow waves, respectively. For $u > c$, a signal applied to the plasma at $z = 0$ travels only in the +z-direction, as in conventional electron beams.

No energy conversion can be found because no coupling to a circuit was provided. We shall construct a model of a circuit that is such that the equations preserve their one-dimensional simplicity, as has been done for the traveling-wave tube (1).

A circuit may be represented by introducing into Eq. 2, in addition to the plasma current density J, a circuit current density J_c caused by a one-dimensional "circuit."

$$\frac{1}{\mu_o}\frac{\partial B}{\partial z} = J + J_c \tag{10}$$

All other equations remain unchanged. In particular, it should be noted that in the force equation (1), the magnetic force density $-JB_o$ remains unchanged, since this is the force density on the plasma only. It is useful to look for a small-signal power theorem to use as an aid in recognizing gain mechanisms. By combining Eqs. 10 and 3, we may obtain the conventional small-signal Poynting theorem.

$$\frac{\partial}{\partial z}\left(-\frac{EB}{\mu_o}\right)+\frac{1}{2}\frac{\partial}{\partial t}\frac{B^2}{\mu_o}+EJ+EJ_c=0 \tag{11}$$

A power theorem is obtained, if we are able to write EJ as a divergence (spatial derivative) of the plasma quantities. Using Eq. 5 to express E and Eq. 1 to express J, we obtain

$$\frac{\partial}{\partial z}\left(-\frac{EB}{\mu_o}+P_p\right)+\frac{\partial}{\partial t}\left(\frac{1}{2}\frac{B_o^2}{\mu_o}+W_p\right)+EJ_c=0 \tag{12}$$

where

$$P_p=(\rho_o v+up)\left(vu+\frac{p}{\rho_o}\right) \tag{13}$$

$$W_p=\rho_o\frac{v^2}{2}+\frac{1}{2}\frac{\rho p}{\rho_o}+\rho vu \tag{14}$$

The quantity P_p is a small-signal power density carried by the plasma, and W_p is a small-signal energy density. From Eq. 11 we find that a time-average power transfer to the circuit may be obtained only by a rate of decrease with distance of the time average of P_p. If we investigate the two waves in the undriven plasma, we find that

$$P_b=\pm\rho_o v^2 c\left(1\pm\frac{u}{c}\right)^2 \tag{15}$$

where the plus sign applies to the fast wave, and the minus sign applies to the slow wave. The slow wave carries negative power. From our experience with coupling of modes (2,3) we conclude that the coupling of a forward circuit wave with the synchronous slow wave must result in a pair of growing and decaying waves. As we see from Eq. 7, the forward-circuit wave can be synchronous with a <u>forward</u> slow wave only for $u > c$; that is, when the dc velocity of the plasma beam is greater than the velocity of the plasma waves. This condition coincides with the condition that an excitation in the plasma at $z = 0$ propagates only in the $+z$-direction so that the growing wave can indeed be excited by an excitation at the input end of the circuit.

To study these conclusions in detail, circuit equations have been devised that are consistent with the assumption of one-dimensionality. They are

$$\frac{dV}{dz} = -j\omega LI + \frac{dV_p}{dz} \tag{16}$$

$$\frac{dI}{dz} = -j\omega CV \tag{17}$$

Here dV_p/dz is the voltage rise per unit length caused by the plasma. The coupling may be thought to be produced by current sheets of unit width in the x- and y-directions,

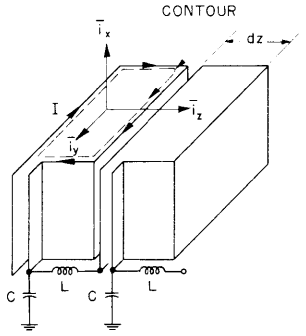

Fig. II-18. The circuit.

as shown in Fig. II-18. The current I in Eqs. 16 and 17 is evaluated per unit width. From this figure we gather that J_c of Eq. 10 is expressible in terms of I as

$$J_c = -\frac{dI}{dz} \tag{18}$$

The voltage dV_p is found from the fact that the complex power change on the circuit within dz must be

$$\frac{1}{2}(I^* dV + V dI^*) = -\frac{1}{2}(j\omega L|I|^2 - j\omega C|V|^2)\, dz + \frac{1}{2} I^* dV_p \tag{19}$$

But the power transferred to the circuit is also given by

$$\frac{1}{2} I^* dV_p = \frac{1}{2} I^* \int_c \bar{E} \cdot d\bar{s} \tag{20}$$

The integral $\int \bar{E} \cdot d\bar{s}$ may be evaluated over a closed contour and the integral converted by Faraday's law. We then have

$$\frac{1}{2} I^* \int_c E \cdot ds = \frac{1}{2} j\omega\mu_o H I^* \tag{21}$$

Comparing Eqs. 21 and 20, we find that

$$\frac{dV_p}{dz} = j\omega\mu_o H \tag{22}$$

Introducing Eq. 22 into Eq. 16 and solving the set Eqs. 1-6 and Eqs. 15-18, with Eq. 2 replaced by Eq. 10, we obtain

$$(\omega - u\beta)^2 - c^2\beta^2 = \frac{B_o^2}{\mu_o \rho_o} \frac{\beta_o^2}{\beta_o^2 - \beta^2} \beta^2 \tag{23}$$

where $\beta_o = \omega\sqrt{LC}$.

A solution of these equations for small coupling (small deviations of β_o and β from $\omega/u + c$ or $\omega/u - c$) gives at synchronism

$$\delta^2 = \pm\beta_o^2 \frac{B_o^2}{\mu_o \rho_o} \frac{\beta_o c}{\omega}$$

with

$$\beta_o = \frac{\omega}{u \pm c} \text{ and } \beta = \beta_o + \delta$$

where plus applies to the fast wave, and minus to the slow wave. The solution shows that gain can indeed be achieved by coupling to the slow wave, provided that β_o is greater than zero; that is, for $u > c$. The coupling is accomplished through the dc magnetic field. Growing waves and thus power amplification at $u > c$ are obtained by coupling to the slow wave (1, 2, 3).

H. A. Haus

References

1. J. R. Pierce, Traveling-Wave Tubes (D. Van Nostrand Company, Inc., New York, 1950).

2. J. R. Pierce, Coupling of modes of propagation, J. Appl. Phys. 25, 179 (1954).

3. H. A. Haus, Electron beam waves in microwave tubes, Symposium Volume, Symposium on Electronic Waveguides, Polytechnic Institute of Brooklyn, April 1958.

6. DYNAMICS OF IONIZED GASES

The theoretical study of plasma dynamics has a propensity for producing equations of formidable complexity. Not the least of these is the hierarchy produced by the multiple integration of the Liouville equation. This linked set has been subjected to a great deal of scrutiny, and numerous methods have been proposed for its solution. The method of interest here is not new (1). It is based on the fact that this linked set can be terminated after the second equation by making an expansion in a small parameter that turns out to be the reciprocal of the number of particles in a Debye sphere. The two resulting equations can then be used to study the dynamics of ionized media. It is the

objective of this study to formulate mathematical methods appropriate for the solution of these equations and to examine some of their properties.

We take as our basic equations

$$\left\{\frac{\partial}{\partial t}+\vec{v}_i\cdot\frac{\partial}{\partial\vec{x}_i}-\frac{e_i}{m_i}\left(\vec{E}_i+\frac{1}{c}\vec{v}_i\times\vec{B}\right)\cdot\frac{\partial}{\partial\vec{v}_i}\right\} f_i(\vec{X}_i)$$

$$=\sum_j\frac{\rho_j e_i e_j}{m_i}\int d\vec{X}_j\,\frac{\partial}{\partial\vec{x}_i}\,\frac{1}{|\vec{x}_j-\vec{x}_i|}\cdot\frac{\partial}{\partial\vec{v}_i}\,F_{ij}(\vec{X}_i,\vec{X}_j) \tag{1}$$

and

$$\left[\frac{\partial}{\partial t}+\vec{v}_i\cdot\frac{\partial}{\partial\vec{x}_i}+\vec{v}_j\cdot\frac{\partial}{\partial\vec{x}_j}-\frac{e_i}{m_i}\left(\vec{E}_i+\frac{1}{c}\vec{v}_i\times\vec{B}\right)\cdot\frac{\partial}{\partial\vec{v}_i}-\frac{e_j}{m_j}\left(\vec{E}_j+\frac{1}{c}\vec{v}_j\times\vec{B}\right)\cdot\frac{\partial}{\partial\vec{v}_j}\right]F_{ij}$$

$$-\frac{\partial f_i}{\partial\vec{v}_i}\cdot\sum_k\frac{\rho_k e_i e_k}{m_i}\int d\vec{X}_k\,\frac{\partial}{\partial\vec{x}_i}\,\frac{1}{|\vec{x}_i-\vec{x}_k|}\,F_{jk}$$

$$-\frac{\partial f_j}{\partial\vec{v}_j}\cdot\sum_k\frac{\rho_k e_j e_k}{m_j}\int d\vec{X}_k\,\frac{\partial}{\partial\vec{x}_j}\,\frac{1}{|\vec{x}_j-\vec{x}_k|}\,F_{ik}$$

$$=e_i e_j\frac{\partial}{\partial\vec{x}_i}\,\frac{1}{|\vec{x}_i-\vec{x}_j|}\cdot\left(\frac{1}{m_i}\frac{\partial}{\partial\vec{v}_i}-\frac{1}{m_j}\frac{\partial}{\partial\vec{v}_j}\right)f_i f_j \tag{2}$$

where

$$E_i=\sum_k e_k\rho_k\int d\vec{X}_k\,\frac{\partial}{\partial\vec{x}_i}\,\frac{1}{|\vec{x}_i-\vec{x}_k|}\,f_k$$

Here, the summations are over all species; $f_i(\vec{X}_i)\,\frac{d\vec{X}_i}{V}$ is the probability of finding a particle of species i in the phase-space volume $d\vec{X}_i = d\vec{x}_i d\vec{v}_i$, with V, the total volume; $\rho_i = N_i/m_i$, with N_i, the total number of particles of type i; and e_i and m_i are the charge and mass of particles of type i.

The validity of these equations rests upon the assumption that the correlation function F_{ij} is small compared with $f_i f_j$. These equations have been investigated by several authors (2, 3, 4). The usual procedure is to solve Eq. 2 for F_{ij} in terms of f_i and f_j, and then insert this expression in Eq. 1. The result is a kinetic equation for f_i.

a. Solution of the Correlation Equation

In solving Eq. 2, we introduce an N^2-dimensional vector (N is the number of species) whose components are the correlation functions $F_{ij}(\vec{X}_1,\vec{X}_2)$:

$$F = \begin{bmatrix} F_{11} \\ F_{12} \\ \vdots \\ F_{1N} \\ F_{21} \\ \vdots \\ F_{2N} \\ \vdots \\ F_{NN} \end{bmatrix}$$

It is now possible to write the entire set, Eq. 2, as a single matrix equation:

$$\frac{\partial F}{\partial t} + \{A_1[a(\vec{X}_1)]+W_1[\gamma(\vec{X}_1)]+A_2[a(\vec{X}_2)]+W_2[\gamma(\vec{X}_2)]\}\, F = S(\vec{X}_1, \vec{X}_2) \tag{2a}$$

where the matrix operators A_1, A_2, W_1, W_2, and the source vector S are defined as follows:

$$W_1(\gamma) = \begin{bmatrix} \gamma_{11}U & \gamma_{12}U & \cdots & \gamma_{1N}U \\ \gamma_{21}U & & & \vdots \\ \vdots & & & \\ \gamma_{N1}U & \cdots & & \gamma_{NN}U \end{bmatrix} \qquad W_2(\gamma) = \begin{bmatrix} T & & & & 0 \\ & T & & & \\ & & T & & \\ & & & T & \\ 0 & & & & \ddots \end{bmatrix}$$

$$U = \begin{bmatrix} 1 & & & 0 \\ & 1 & & \\ & & 1 & \\ 0 & & & \ddots \end{bmatrix} \qquad T = \begin{bmatrix} \gamma_{11} & \gamma_{12} & \cdots & \gamma_{1N} \\ \gamma_{21} & & & \vdots \\ \vdots & & & \\ \gamma_{N1} & \cdots & & \gamma_{NN} \end{bmatrix}$$

$$\gamma_{ij}(\vec{X}_1) = -\frac{\rho_j e_i e_j}{m_i} \frac{\partial f_i(\vec{X}_1)}{\partial \vec{v}_1} \cdot \int d\vec{X}_1' \frac{\partial}{\partial \vec{x}_1} \frac{1}{|\vec{x}_1' - \vec{x}_1|}$$

and similarly for $\gamma(\vec{X}_2)$. The integral operator $\gamma_{ij}(\vec{X}_1)$ is intended to operate only on the $\vec{X}_1$ coordinate. In other words, if $h(\vec{X}_1, \vec{X}_2)$ is any function of $\vec{X}_1$ and $\vec{X}_2$, then

$$\gamma_{ij}(\vec{X}_1)\, h(\vec{X}_1, \vec{X}_2) = -\frac{\rho_j e_i e_j}{m_i} \frac{\partial f_i(\vec{X}_1)}{\partial \vec{v}_1} \cdot \int d\vec{X}_1'\, h(\vec{X}_1', \vec{X}_2) \frac{\partial}{\partial \vec{x}_1} \frac{1}{|\vec{x}_1' - \vec{x}_1|}$$

The A matrices are given by

$$A_1[a] = \begin{bmatrix} a_i U & & & 0 \\ & a_2 U & & \\ & & a_3 U & \\ 0 & & & a_N U \end{bmatrix} \qquad A_2[a] = \begin{bmatrix} R & & & 0 \\ & R & & \\ & & R & \\ 0 & & & \end{bmatrix}$$

$$R = \begin{bmatrix} a_1 & & & 0 \\ & a_2 & & \\ & & \ddots & \\ 0 & & & a_N \end{bmatrix}$$

where

$$a_i(\vec{X}_1) = \vec{v}_1 \cdot \frac{\partial}{\partial \vec{x}_1} - \frac{e_i}{m_i}\left(\vec{E}(\vec{X}_1) + \frac{1}{c}\vec{v}_1 \times \vec{B}(\vec{X}_1)\right) \cdot \frac{\partial}{\partial \vec{v}_1}$$

Finally, the source vector is defined by

$$S = \begin{bmatrix} s_{11} \\ s_{12} \\ \vdots \\ s_{1N} \\ \vdots \\ s_{NN} \end{bmatrix}$$

where

$$s_{ij} = e_i e_j \frac{\partial}{\partial \vec{x}_1} \frac{1}{|\vec{x}_1 - \vec{x}_2|} \cdot \left(\frac{1}{m_i}\frac{\partial}{\partial \vec{v}_1} - \frac{1}{m_j}\frac{\partial}{\partial \vec{v}_2}\right) f_i(\vec{X}_1)\, f_j(\vec{X}_2)$$

If we now define the operators

$$H_1(\vec{X}_1) = A_1[a(\vec{X}_1)] + W_1[\gamma(\vec{X}_1)]$$

$$H_2(\vec{X}_2) = A_2[a(\vec{X}_2)] + W_2[\gamma(\vec{X}_2)]$$

$$H = H_1 + H_2$$

Eq. 2a becomes simply

$$\frac{\partial F}{\partial t} + HF = S \tag{2b}$$

The solution of Eq. 2b is given by

$$F = P(t) \int_0^t P^{-1}(\tau)\, S(\tau)\, d\tau + P(t)\, F^o \tag{3}$$

where P(t) is an operator that obeys the equation

$$\frac{\partial P}{\partial t} + HP = 0 \tag{4}$$

It is not difficult to show that H_1 and H_2 commute, so that Eq. 4 can be separated into the two equations

$$\frac{\partial P_1}{\partial t} + H_1 P_1 = 0 \text{ and } \frac{\partial P_2}{\partial t} + H_2 P_2 = 0 \tag{5}$$

where

$$P(\vec{X}_1, \vec{X}_2, t) = P_1(\vec{X}_1, t)\, P_2(\vec{X}_2, t)$$

Power series solutions to Eq. 5 can be developed, but they appear to be of limited usefulness. For many plasmas of interest, a more tractable method is possible.

b. The Adiabatic Hypothesis

Let us assume that the two-particle functions F_{ij} relax and come into equilibrium with the one-particle function f_i in a time so short that f_i will not have changed very much. Then we may neglect the time dependence of H and write the solution of Eq. 4 as

$$P = P_1 P_2 = e^{-Ht} = e^{-H_1 t}\, e^{-H_2 t} \tag{6}$$

and therefore

$$F = \int_0^t e^{-H\tau} S(t-\tau)\, d\tau + \exp(-Ht)\, F^o \tag{7}$$

The operators P_1 and P_2 have a rather simple interpretation in the adiabatic hypothesis. A study of Eqs. 5 shows that the application of $P_1(t)$ to an arbitrary function $h(\vec{X}_1)$ produces a time-dependent function that satisfies the linearized Vlasov equation and whose intitial value is $h(\vec{X}_2)$. An analogous statement holds for P_2.

Now we can understand what Eq. 7 means. Formally, it corresponds to the solution

of a reservoir problem in which the reservoir, whose level is F(t), is fed by a source S(t) and depleted by a leakage -HF(t).

In our problem the correlation "level" is fed by the Coulomb repulsion between particles which produces a flow, $S(\tau)$ into (or out of) volume elements for which $|\vec{x}_i - \vec{x}_j|$ is small. The "leakage" comes from the operators P_1 and P_2, which try to iron out the resulting inhomogeneity by Landau damping action.

For those velocity distributions that lead to sufficiently rapid damping in the Vlasov equation (analogous to large H), we would expect the correlation function F to depend very little on past values of S(t), or therefore of $f_i(t)$. Also the initial value of F should damp out rapidly and become unimportant. In such a case we are justified in using the adiabatic hypothesis. The expression for F becomes simply

$$F = \int_0^\infty P_1(\tau)\, P_2(\tau)\, S(t)\, d\tau$$

Substitution of this expression in Eq. 1 produces the kinetic equation for f_i, which turns out to be a Fokker-Planck equation.

When f_i is considered constant in time, the equations for P_1 and P_2 can be easily solved by Fourier and Laplace transform methods. For example, in a homogeneous plasma with B = 0, the transform of $P_1 h$ is

$$(P_1 h)_{s,\vec{k}} = -W_1(\psi)\left[I + \int d\vec{v}\, W_1(\psi)\right]^{-1} \int \frac{(h)_{\vec{k}}}{s - i\vec{k}_1 \cdot \vec{v}_1}\, d\vec{v} + \frac{(h)_{\vec{k}}}{s - i\vec{k}_1 \cdot \vec{v}_1}$$

where

$$\psi_{ij} = \frac{4\pi \rho_j e_i e_j}{m_i} \frac{\partial f_i(\vec{X}_1)}{\partial \vec{v}_1} \cdot \frac{i\vec{k}_1}{k_1^2} \frac{1}{s - i\vec{k}_1 \cdot \vec{v}_1}$$

For those velocity distributions that do not lead to rapid damping, the adiabatic hypothesis is inapplicable, and the solution of the correlation equation becomes more involved. Indeed, for those distributions that lead to instabilities in the Vlasov equation, it appears that an entirely new regime develops in F. Not only does F not come into equilibrium with f_i; it grows exponentially as compared with f_i, until finally our perturbation scheme breaks down altogether. It is impossible to tell with this method what the ultimate effect of the instability on F is. However, preliminary calculations indicate that F does grow in such a way that the collision term relaxes the velocity distribution toward a more stable one.

The adiabatic hypothesis also seems unsuitable for treating plasmas with large macroscopic inhomogenieties. The relaxation mechanism of the P operators is that of Landau

damping and hence occurs in a time whose magnitude is of the order of the reciprocal plasma frequency. But unfortunately this is the same time scale associated with macroscopic behavior. Thus we cannot assume that correlation processes occur in a time so short that f_i does not change.

T. H. Dupree

References

1. N. Bogoliubov, Problems of Dynamical Theory in Statistical Physics (State Technical Press, Moscow, 1946).

2. B. B. Kadomtsev, Soviet Phys. – JETP 6, 117 (1958).

3. C. M. Tchen, Phys. Rev. 114, 394 (1959).

4. N. Rostoker and M. N. Rosenbluth, Phys. Fluids 3, 1 (1960).

7. PRELIMINARY DESCRIPTION OF EXPERIMENTAL APPARATUS TO BE USED IN PLASMA DIFFUSION STUDY

During the past quarter, the research effort was concentrated on the design and construction of probes, and their associated fixtures, circuitry, and recording devices that will soon be used to study diffusion across a magnetic field in the plasma produced by the hollow-cathode discharge (1).

a. Probes

The probe design is shown in Fig. II-19. The sphere on the end of the tungsten rod is made by helium-arc welding and then polishing. If a plane probe is desired, the original sphere can be ground to a hemisphere and coated with Al_2O_3 except for the plane face. These probes have been tested at the center of the hollow-cathode discharge, and the Al_2O_3 appears to withstand the high temperature. Glass-insulated probes are unsuitable because the glass melts.

The probe has been operated for six-hour periods with no sign of increasing the effective collection area because of deposits from the cathode. Visual examination of the probe, after operation, showed a darkening of the white Al_2O_3 coating that may have been caused by a tantalum deposit. However, the rough texture of the Al_2O_3 coating seems to prevent the formation of a conducting path.

b. Flexible Vacuum Seals

The flexible vacuum seal, designed to be mounted onto the wall of the vacuum chamber, for use with the probes just described is shown in Fig. II-20. This ball-and-socket joint allows an in-and-out motion through the O-ring of 1/8-inch diameter (Fig. II-20a), as well as an angular rotation of 90°. The ball and socket is interchangeable so that

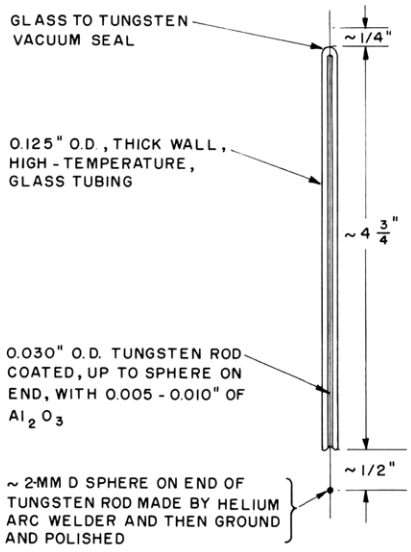

Fig. II-19. Al_2O_3-coated tungsten probe.

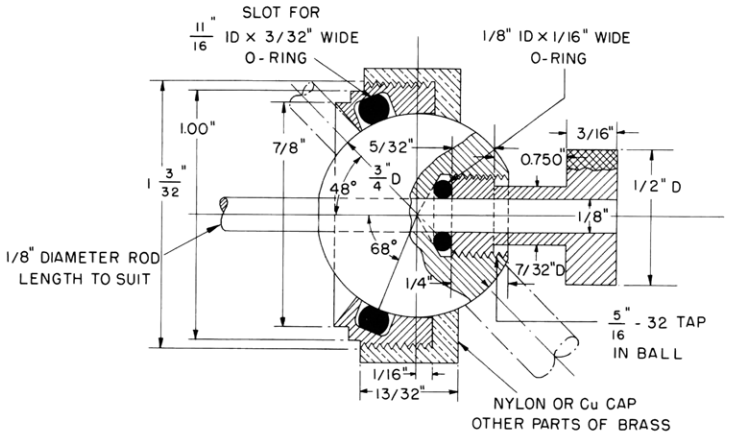

Fig. II-20. Flexible vacuum probe unit.

another ball, with a larger hole, can be substituted to admit a larger sized rod for other purposes. The assembly has been vacuum-tested at 10^{-5} mm Hg and will execute the full range of rotary in-and-out motion with no detectable leaks. In fact, the screw caps can be loosened completely, and the external pressure on the O-rings is sufficient to maintain the vacuum seal. This assembly allows the probe to be positioned in almost any part of the plasma region while the discharge is in operation. (For further details and working drawings see RLE DWG. B-1947 A-E.)

c. Circuit

The circuit that will be used to take probe data is shown in Fig. II-21. It is designed for dc operation in conjunction with an X-Y recorder. The probe voltage is swept

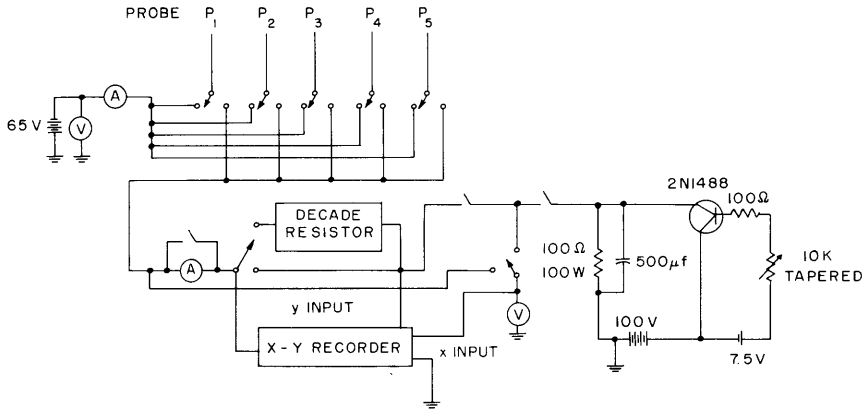

Fig. II-21. Probe circuit.

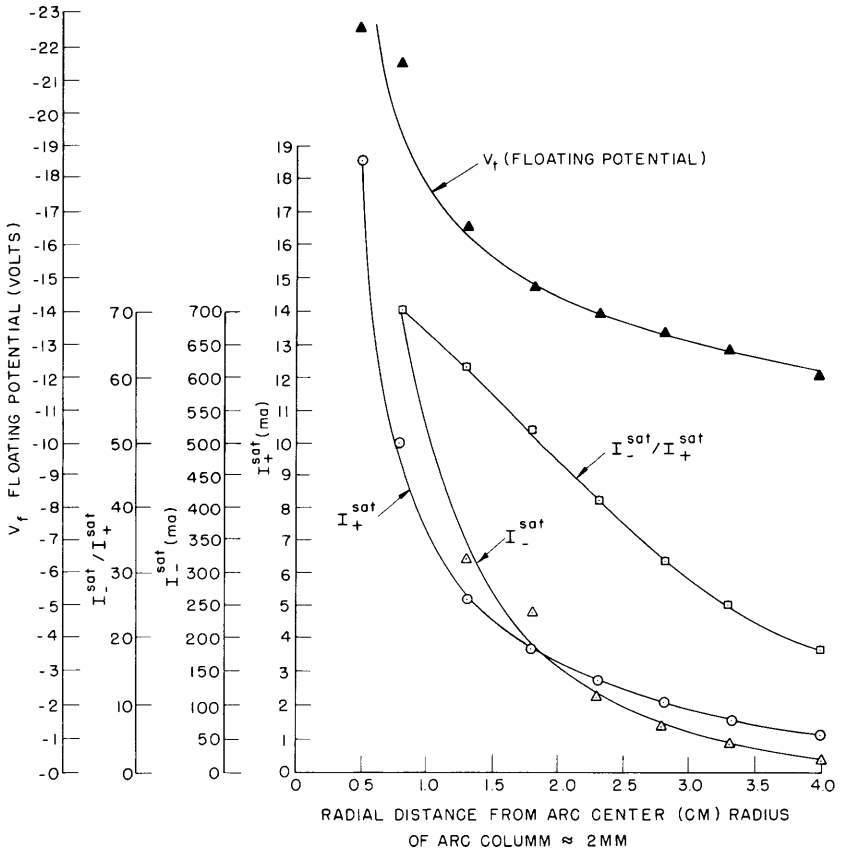

Fig. II-22. Radial profiles taken with Langmuir probe in hollow-cathode discharge (1/8-inch diameter) with argon gas. Probe area, approximately 3 mm^2; voltage measurements made with respect to grounded anode.

manually by varying the 10-K rheostat. The 65-volt battery maintains those probes that are not in immediate use, at large negative potential so that ion bombardment will keep their surfaces clean.

d. Preliminary Data

The preliminary data presented in Fig. II-22 were taken in the course of testing the Al_2O_3-coated probes. This figure shows radial distributions of floating potential (V_f), and ion and electron saturation current. A conducting wall is located at a radius of approximately 5 cm. Note that the floating potential at the center of the plasma is more negative than it is at the wall. This is partially due to the fact that the Larmor radius for electrons is 0.1 mm, while that for A^+ ions is 4 cm. Also note that the ratio of electron-to-ion saturation current varies from 20 to 70, instead of having the value approximately 270, which is $\left(\frac{M(A^+)}{m_e}\right)^{1/2}$, as predicted by simple Langmuir probe theory. If the plasma temperature is constant across the radius, then the saturation-current curves are proportional to the density.

S. D. Rothleder

References

1. D. J. Rose, L. M. Lidsky, S. D. Rothleder, and S. Yoshikawa, Experimental results on the hollow-cathode discharge, Quarterly Progress Report No. 58, Research Laboratory of Electronics, M.I.T., July 15, 1960, pp. 41-44.

8. ELECTRON-BEAM TRAPPING

A recent experiment at this laboratory has demonstrated the total trapping of a beam of electrons injected axially into a time-invariant pair of magnetic mirrors. The novel feature of the experiment was the creation of helically twisted magnetic-field lines in the region between the mirrors in such a manner that the pitch of the field closely matched the pitch of the electron trajectories at all points during the initial traverse of the electrons between mirrors.

Theory suggests that practical application of this effect will be limited to situations in which $0.2 < r_c/r_o < 0.6$, where r_c is the cyclotron radius of a particle of the injected energy moving in a plane perpendicular to the axial B field, and r_o is the radius of the structure producing the twisted field. Larger values of r_c/r_o may be useful in applications in which decreasing the magnetic moment of particles in a beam is desired, for example, before bringing a beam out of a region of high magnetic field.

Thus far, for the sake of simplicity and convenience, magnetic-field shaping has been done only with iron helices, and work has been restricted to axial fields of a few

hundred gauss. For fields in the kilogauss range, iron would not be suitable, therefore long pitch helical current carrying windings would be required.

a. Theory

The essential features of the synchronous trapping can be obtained from an approximate solution of the equations of motion in cylindrical coordinates and in the presence of a magnetic field.

$$r'' - r\theta'^2 = \frac{q}{m}(B_z r\theta' - B_\theta z')$$
$$r\theta'' + 2r'\theta' = \frac{q}{m}(B_\theta z' - B_z r') \tag{1}$$

$$z'' = \frac{1}{2}\frac{d}{dz}(z')^2 = \frac{q}{m}(B_\theta r' - B_r r\theta') \tag{2}$$

$$r'^2 + r^2\theta'^2 + z'^2 = v_o^2 \tag{3}$$

Primes indicate derivatives with respect to time. The phenomena to be described is the slow increase in the transverse energy component of a beam of particles with initial velocity v_o in the z direction. If the beam is initially along the z-axis, then the motion of the particles at any time can be described approximately by a circular component around, and a translation along, the z-axis. If the circular component is changing slowly, then it is reasonable to neglect r' in Eqs. 2 and 3. Eliminating $r\theta'$ yields the relation

$$\frac{d}{dz}(z')^2 = 2\left|\frac{q}{m}\right| B_r\left(v_o^2 - z'^2\right)^{1/2} \tag{4}$$

The B_r in this equation is that at the instantaneous particle position. A conventional magnetic mirror causes $(z')^2$ to be decreased by creating a negative B_r in the entire mirror region. In this case, of course, magnetic moment happens to stay constant. Another possibility is to establish the path that the beam will follow and to arrange that B_r be negative only along that path. This can be achieved by twisting of the B lines with no over-all increase in the strength of the field. In this case magnetic moment will increase. B_r must be related to either z or z' to permit solution of Eq. 4. From geometric considerations one would expect that feasible values of B_r would be smaller for a short-pitch helix than for a long-pitch helix. Some insight into the nature of the solution can be obtained by assuming that

$$B_r = B_{r_o}\left(\frac{z'}{v_o}\right)^n \tag{5}$$

For any integer n the solution may be obtained explicitly, and z'/v_o will be a function of the variable

$$S \equiv \frac{q}{m}\frac{B_{r_o}}{v_o} z = \frac{w_c}{v_o}\frac{B_{r_o}}{B_z} z = \frac{B_{r_o}}{B_z}\frac{z}{r_c} \tag{6}$$

where w_c and r_c are the cyclotron frequency and radius obtained from Eq. 1 for $r'' = z' = 0$. In terms of this variable the series expansions of the solutions to Eqs. 4 and 5 start off as

$$\left(\frac{z'}{v_o}\right)^2 = 1 - S^2 + \ldots \tag{7}$$

For a practical trapping system it is sufficient to make $(z'/v_o)^2 = 1/2$, since this would permit reflection by a conventional mirror with mirror ratio of 2. Examination of a number of solutions of Eq. 4 shows that a sufficient condition for a workable synchronous mirror is that

$$S_{1/2} = \frac{B_{r_o}}{B_z}\frac{L}{r_c} = 1 \tag{8}$$

This gives the necessary length, L, of the synchronous region. It remains to determine feasible values for B_{r_o}/B_z.

A twisted B-field may be obtained in several ways. Most configurations, including the most practical ones, are not susceptible to analysis. As a result, two idealized cases will be considered: one involving currents; and the other, magnetic material.

Consider an infinitely long conducting ribbon wound into a helix with uniform pitch p and radius r_o and carrying a current J. Let w/p be the fraction of cylinder surface covered by the ribbon. Straightforward integration of the Biot-Savart law for the field on the axis of the helix (mks units) gives

$$B_z = \frac{\mu_o J}{p}$$

$$\begin{Bmatrix} B_r \\ B_\theta \end{Bmatrix} = \frac{\mu_o J}{p} \begin{Bmatrix} \sin \\ \cos \end{Bmatrix} \left(\frac{2\pi z}{p} - \theta\right) \left[\frac{\sin\left(\frac{\pi w}{p}\right)}{\left(\frac{\pi w}{p}\right)}\right] \left[\frac{r_o}{r_c} K_o\left(\frac{r_o}{r_c}\right) + K_1\left(\frac{r_o}{r_c}\right)\right]$$

where z and θ are the field coordinates with origin at a radius line passing through the center of the conducting ribbon, and the K's are Hankel functions. If desired, this expression is readily integrated with respect to r_o to allow for a coil of finite thickness as well as width. For the case considered here, it is apparent that

$$\frac{B_r}{B_z} \leq \frac{r_o}{r_c} K_o\left(\frac{r_o}{r_c}\right) + K_1\left(\frac{r_o}{r_c}\right) \tag{9}$$

This relation is plotted in Fig. II-23.

Only a very crude analysis of the case for magnetized material has thus far been undertaken. Consider a ribbon of magnetized material of thickness t wound into a helix

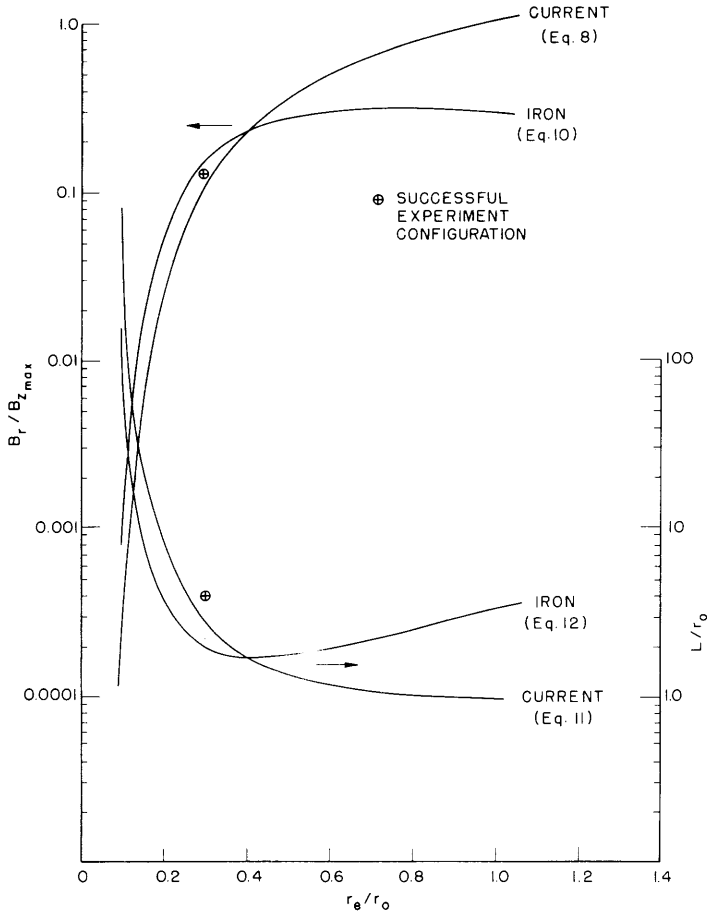

Fig. II-23. Design consideration for synchronous trapping.

with uniform pitch p and radius r_o and having a uniform magnetization $\overline{M}$ parallel to the axis of the helix. Let w/p be the fraction of cylinder surface covered by the ribbon. The scalar magnetic potential for such a structure will be given by

$$\phi_m = \frac{1}{4\pi} \int \frac{\vec{M} \cdot \vec{ds}}{|\overline{R}|}$$

and the expressions for the field on the axis of the helix (which are valid for $t/r_o \ll 1$)

will be given by

$$\left.\begin{aligned} B_z &= 0 \\ \left\{\frac{B_r}{B_\theta}\right\} &\approx \left(\frac{M}{\pi}\right)\left(\frac{t}{r_o}\right)\left\{\begin{matrix}\sin\\ \cos\end{matrix}\right\}\left(\frac{2\pi z}{p}-\theta\right)\ \sin\left(\frac{\pi w}{p}\right)\left[\left(\frac{r_o}{r_c}\right)^2 K_1\left(\frac{r_o}{r_c}\right)\right] \end{aligned}\right\} \tag{10}$$

When iron is used in the helix, M is not uniform and is a function of B_z, t, and W. For the experiments reported here, $\mu_o M \approx 3000$ gauss, $t/r_o \approx 0.25$, $W/t \approx 4$, and $B_z \approx$ 500 gauss. Thus

$$\frac{B_r}{B_z} \leq \frac{1}{2}\left(\frac{r_o}{r_c}\right)^2 K_1\left(\frac{r_o}{r_c}\right) \tag{11}$$

This relation is also plotted in Fig. II-24. Substitution of Eq. 9 or Eq. 11 in Eq. 8 gives:

For current,

$$\frac{r_o}{L} = \left(\frac{r_o}{r_c}\right)^2 K_o\left(\frac{r_o}{r_c}\right) + \left(\frac{r_o}{r_c}\right) K_1\left(\frac{r_o}{r_c}\right) \tag{12}$$

and for iron,

$$\frac{r_o}{L} = \frac{1}{2}\left(\frac{r_o}{r_c}\right)^3 K_1\left(\frac{r_o}{r_c}\right) \tag{13}$$

These equations are also plotted in Fig. II-24. The large point plotted in the figure represents the actual measured values for the final experimental trapping configuration. The curves for iron can obviously be shifted vertically by changing the iron thickness. The current curves could also be shifted if a power-wasting coil configuration were used. By winding a second current ribbon in the space left by the first but with current flowing in the opposite direction, one can increase B_r while decreasing B_z.

In a trapping experiment it will be desirable to have $r_c/r_o \leq 1$, and preferably much smaller. On the other hand, it is apparent from the plots that no significant synchronous effect can be achieved for $r_c/r_o < 0.1$. This conclusion is so strongly indicated by the idealized analysis that it is probably valid for more realistic cases and the range of interest is most likely within a factor of 2 from the value $r_c/r_o = 0.3$.

b. Experiment

In the successful trapping experiment the twisted field was created by an iron helix of variable pitch. The helix was constructed from a piece of mild steel bar stock, 1/8 inch thick by 30 inches long and tapered into a cosine, with a width of 0.5 inch at the

center and zero at each end. This bar was wound into a helix of 1-inch inside diameter with a pitch length of 1 inch at the center and decreasing in an esthetically pleasing manner to each end. The final structure was approximately 4 inches long.

This structure satisfies the solution of Eq. 4 for the case where n = 0 in Eq. 5. The value n = 0 is not realistic, but this is the only value that results in a helix that can be wound from a bar of finite length with zero width at the end. It is necessary that the bar taper to zero; otherwise the asymmetry created by the end causes the electron beam to be deflected from its initial axial position, an effect that might mask the synchronous effect. The helix is constructed symmetrically about the center for the same reason, the first half merely serves as an inlet structure to avoid spurious beam perturbations.

The length of the effective part of the structure was made approximately twice as long as that required by Eq. 8. This provides a mechanism for phase stability of the beam trajectory. As shown in Eq. 10, for a given θ the value of B_r seen by the particle will depend on its position z. The iron helix was shaped to require that $\frac{2\pi z}{p} - \theta \approx \pi/6$. If z' is larger than it should be at any point, then z will increase faster than it should; thus B_r will increase (negatively) and deceleration will increase and the particle will tend to return to the design trajectory. Similarly, if z' is too small, the particle will be decelerated less and will tend to catch up.

Figure II-24 shows the axial B_z of the experiment, as well as the locations of the

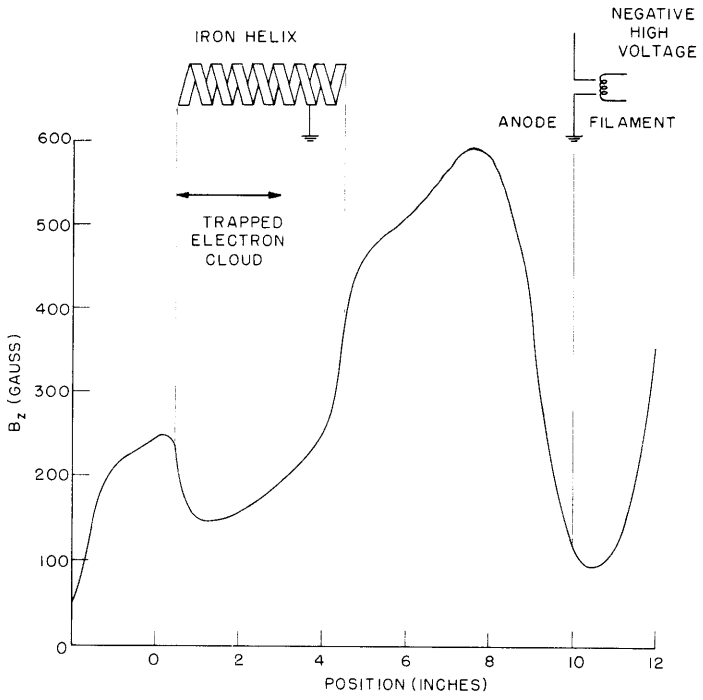

Fig. II-24. Experimental configuration.

electron gun and the iron helix. No care was taken in shaping the field. A large solenoid with a variable current supply was available and the perturbations in the field were made with some pieces of iron pipe which happened to be handy. The various iron pieces and the electron gun were carefully aligned and placed inside a glass pipe, 4 inches in diameter, attached to a vacuum system and penetrating the solenoid.

The system pressure was maintained at approximately 1 μ to permit visual observation of the electron beam. The electron gun would deliver a few hundred microamperes at 0 to 1000 volts, and the maximum B_r/B_z ratio was measured to be 0.13 nearly independent of B_z over the range of interest. The mirror for initial reflection had a ratio less than 2 (approximately 1.6).

Visual observation confirmed all predictions of theory. The beam from the electron gun was of less than 1/8-inch diameter (1/16 inch at some B-fields) on axis, and had no discernible angular component. For values of voltage and B_z that gave a value of r_c/r_o far removed from 0.3 in any direction, the beam was only slightly perturbed on passing through the system, and no trapping occurred. As the value $r_c/r_o = 0.3$ was approached, the beam became a helix matching the pitch of the iron helix. In this condition the beam took on a flat ribbonlike appearance that was probably caused by the phase-stabilizing action of the field and a velocity dispersion of the beam. As optimum resonance condition was attained, the beam was totally reflected and organized trajectories within the iron helix were obscured by the diffuse glow of ionization by the trapped electrons. Close observation of the beam just before this condition was reached did not show any part of the beam approaching any solid surface. Thus the stopping of the beam is not due to deflection into a wall. If the solenoid current is reversed, then the helical paths of the particles will have an opposite twist from that of the iron helix. Under these conditions, a value $r_c/r_o = 0.3$ caused the beam to be slightly perturbed, but no trapping occurred under any conditions.

This work arose out of attempts to control the electron-energy distribution in a nonequilibrium plasma. The trapping technique might well have application in the thermonuclear program, however. An example might be in the DCX machine in which elimination of the large arc now used for ion trapping would solve several problems.

R. C. Wingerson

9. TRANSPORT COEFFICIENTS CALCULATED FROM THE LIOUVILLE EQUATION

The satisfactory treatment of collision effect in plasma is necessary for the understanding of diffusion, conductivity, and thermalization. Two approaches have previously been made: by the Boltzmann integral method (1), and by the stochastic method (2). Although both explain the observable phenomena amazingly well, the assumptions are somewhat too axiomatic. A different approach has been proposed by Bogoliubov (3). It

has been successfully applied to plasma physics, notably by Rostoker and Rosenbluth (4). The approach in this report was made in slightly different fashion, in order to get physical quantities without introducing the assumption of a test particle.

The starting point is the 6N-dimensional Liouville equation,

$$\frac{Df}{Dt} = \frac{\partial f}{\partial t} + [f, H] \tag{1}$$

in which the bracket is the Poisson bracket. From the assumption that the potential energy of each particle is small compared with the kinetic energy of each particle, we can make an expansion of the smallness parameter that is essentially the ratio of potential energy to kinetic energy. To first order, we obtain two sets of equations. One is the equation of a one-body distribution function, which we shall call simply "distribution function." The second is a two-body distribution function, which we shall call "correlation function." After introducing the natural units for this system, that is,

$$q = xn^{1/3}, \quad p = \frac{mv}{\sqrt{2mkT}}, \quad \tau = \omega_p t \tag{2}$$

we get, after Fourier analysis,

$$\frac{\partial f_1}{\partial t_o} + \frac{\epsilon}{4\pi_o}\vec{E}\frac{\partial f}{\partial p} + \lambda(\vec{p}_1 \times \vec{e}_z) = (-i)\,\epsilon \frac{\partial}{\partial \vec{p}_1}\left(\int dp_2 \int \frac{\vec{k}}{k^2} a_k d\vec{k}\right) \tag{3}$$

$$\frac{\partial a_k}{\partial t} + \frac{1}{\epsilon} i\vec{k}(\vec{p}_1 - \vec{p}_2)\, a_k = i\vec{k}\frac{1}{k^2}\epsilon\left[\frac{1}{8\pi^3}\left(\frac{\partial f_1}{\partial \vec{p}_1} f_2 - \frac{\partial f_2}{\partial \vec{p}_2} f_1\right)\right.$$
$$\left. + \left(\frac{\partial f_1}{\partial \vec{p}_1}\int dp_3\, a_{-k_{23}} - \frac{\partial f_2}{\partial \vec{p}_2}\int a_{k_{13}} dp_3\right)\right] \tag{4}$$

$$\left.\begin{aligned} E &= \frac{\vec{E}}{\frac{e}{4\pi\epsilon_o} n^{2/3}}, \quad \lambda = \frac{\omega_e}{\omega_p}, \quad \omega_e = \frac{eB}{m_1} \\ &\left(\frac{\epsilon E}{4\pi}, \lambda \leq 1\right) \end{aligned}\right\} \tag{5}$$

where a_k is the Fourier component of the correlation function in space; f_1, f_2 are distribution functions of argument p_1 and p_2; ϵ is the interatomic distance divided by the Debye shielding length. These are for one species and are uniform in space. The second condition is later relaxed to require spatial inhomogeneity to occur in lengths greater than the Debye length.

We replace a_k by $a_{k_o} f_1 f_2 / f_{10} f_{20}$, where the subscript zero denotes the stationary state. Thus f_{10} is a Maxwellian distribution function. This assumption is the same assumption as that the deviation of the function f from equilibrium is small. Then if f_1 and f_2 change slowly with time, we can express the right-hand side of Eq. 3 in the form of a Fokker-Planck equation:

$$\epsilon^3 \frac{\ln \Lambda}{8\pi} \frac{\partial}{\partial p_1} \int dp_2 \left(\frac{\partial f_1}{\partial p_1} f_2 - \frac{\partial f_2}{\partial p_2} f_1 \right) \left(\frac{d}{dp_1} \cdot \frac{d}{dp_1} \right) |p_1 - p_2|$$

$$= - \frac{\epsilon^3 \ln \Lambda}{4\pi} \left[\frac{\partial}{\partial p_1} \cdot f \frac{\partial}{\partial p_1} h - \frac{1}{2} \frac{\partial}{\partial p_1} \frac{\partial}{\partial p_1} : f \frac{\partial}{\partial p_1} \frac{\partial}{\partial p_1} g \right] \tag{6}$$

where

$$h = 2 \int d\vec{p}_1 \, f(\vec{p}_2) \frac{1}{|p_1 - p_2|} \tag{7}$$

$$g = \int d\vec{p}_2 \, f(\vec{p}_2) \frac{1}{|p_1 - p_2|} \tag{8}$$

The first expression corresponds to one given by Landau from the Boltzmann equation (5), and the second to one given by Rosenbluth (6). Solution of Eq. 6 was tried by expanding f with Hermite polynomials that have been used by some authors for gas kinetic theory (7). Actually, the expansion can be written

$$f = \sum C_n \left(\frac{\vec{\partial}}{\partial p} \right)^n \frac{1}{(\sqrt{\pi})^3} \exp(-\vec{p}^2) \tag{9}$$

where C_n is the tensor of n^{th} rank; C_1 is proportional to velocity; C_2 is related to the pressure tensor; and C_3 is related to the heat-flux tensor.

The first check was made to calculate the temperature relaxation of two different species at different temperatures. The result can be expressed as

$$\frac{d}{dt} T_e = \frac{T_i - T_e}{t_{eq}}, \quad t_{eq} = \frac{3\pi^2}{2\sqrt{\pi}} \frac{1}{\epsilon^3 \ln \Lambda \, \omega_p} \frac{\sqrt{m}}{(\sqrt{T_e})^3} M \left(\frac{T_e}{m} + \frac{T_i}{m} \right)^{3/2} \tag{10}$$

If allowance is made for differences in notation, Eq. 10 coincides with the result obtained by Spitzer (8), who used an ordinary two-body encounter model. Temperature relaxation of parallel and perpendicular components of one species inside the magnetic field was calculated for the case in which cyclotron frequency is less than plasma frequency. We introduce T_o as the reference temperature,

$$\frac{d}{dt}\left(\frac{T_{||}}{T_o}\right) = \frac{2\sqrt{2\pi}}{15\pi^2}\epsilon^3 \ln\Lambda\left(\frac{T_o}{T_{||}}\left(\frac{T_\perp}{T_{||}} - 1\right) I\left(\frac{T_\perp}{T_{||}}\right)\right)^{1/2} \tag{11}$$

$$I(x) = \int_{-1}^{1} d\mu \frac{15}{4}\mu^2(1-\mu^2) \frac{1}{(x+\mu^2(1-x))^{3/2}} \qquad I(1) = 1 \tag{12}$$

If f_1 is time-dependent with fixed frequency, it is possible to calculate the collision term, provided that the deviation from equilibrium is small. More precisely, if the applied field is expressed in natural units, we can write

$$\frac{\epsilon E}{\omega} < 1 \tag{13}$$

This turns out to be not a very stringent condition. The only effect of ω is found inside the logarithmic term which requires that Λ be replaced by $\Lambda\frac{\omega_p}{\omega}$, whenever $\omega > \omega_p$. This condition is rarely observed in a laboratory system because the plasma frequency is too high. But in the ionosphere, this effect can be observed because of low density. Besides, with a different frequency it is possible to determine the coefficient of the logarithmic term from the slope of the collision frequency. The coefficient is proportional to $(n/T^3)^{1/2}$. Hence, it may be used to determine the temperature. The fact that Λ is replaced by $\Lambda\frac{\omega_p}{\omega}$ can be applied to the determination of the properties of the upper atmosphere by measuring the attenuation of electromagnetic waves of different frequencies, say, from an artificial satellite. Strictly speaking, we are not permitted to make ω equal to zero. But in case $\omega \to 0$ the result is the same as the value derived by

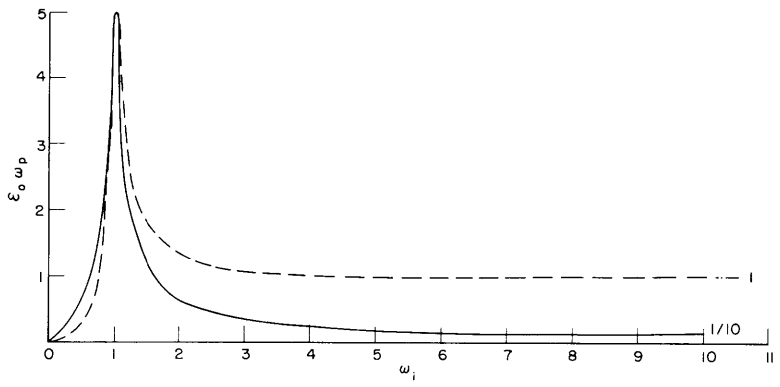

Fig. II-25. Curve of the absolute value of $J = \sigma E$. The dashed line represents the off-diagonal element of the conductivity tensor; the straight line, the diagonal element $\left(\omega_e = \omega_p;\ \nu_c = \frac{1}{10}\omega_p;\ \mu^2 = \frac{m}{M} = \frac{1}{1800}\right)$.

Spitzer (9), and more recently by Kelly (10) in the absence of magnetic field. For this report the general features of the conductivity were calculated. The result is too complicated to reproduce here, but one of the results is shown in Fig. II-25. Note that there is no conductivity when ω equals zero. The electric field is applied perpendicular to the magnetic field. The plasma is assumed to be uniform. The asymptotic value is the same as that calculated when we assume that the ions are immobile.

Wave propagation was calculated for plane and linearized cases. The physical parameters, such as temperature, collision frequency, and the direction of the magnetic field were taken into account. The matrix, which is a generalization of Oster's (11), gives all of the waves that are known to exist in a magnetized plasma.

The derivation of a conventional magnetohydrodynamic relation was tried. The calculation can be carried out by the expansion of Eq. 9. The first-order expansion results in a conventional magnetohydrodynamic equation with collision terms. In conventional notation, we have

$$M\frac{\partial \Gamma_+}{\partial t} + \nabla \cdot p_+ - en\vec{E} - e(\Gamma_+ \times \vec{B}) = -mv_c(\Gamma_+ - \Gamma_-) \tag{14}$$

$$m\frac{\partial \Gamma_-}{\partial t} + \nabla \cdot p_- + en\vec{E} + e(\Gamma_- \times \vec{B}) = +mv_c(\Gamma_+ - \Gamma_-) \tag{15}$$

Note that the right-hand sides of these equations, which represent the collision terms, have the same magnitude but opposite sign. The second-order approximation has an effect through the pressure tensor and change in the scalar number of the collision frequency. These results were applied to explain the Penning Ionization Gauge (PIG) discharge. Our result showed that it is almost impossible with this kind of approach to account for the large current drawn by electrodes. The theory of PIG discharge was formulated in order to explain the large current as a result of the nonlinear effect of diffusion caused by the fluctuation of the electric field (12).

S. Yoshikawa

References

1. S. Chapman and T. G. Cowling, The Mathematical Theory of Non-Uniform Gases (Cambridge University Press, London, 1958).

2. S. Chandrasekhar, Revs. Modern Phys. 15, 1 (1943).

3. C. Tchen, Phys. Rev. 114, 394 (1959).

4. N. Rostoker and M. N. Rosenbluth, Phys. Fluids 3, 1 (1960).

5. J. Enoch, Phys. Fluids 3, 353 (1960).

6. M. N. Rosenbluth, W. M. MacDonald, and D. L. Judd, Phys. Rev. 107, 350 (1957).

(References continued on following page)

7. A. Sommerfeld, Thermodynamics and Statistical Mechanics (Academic Press, Inc., New York, 1956).

8. L. Spitzer, Jr., M. N. Roy. Astron. Soc. 100, 396 (1940).

9. L. Spitzer, Jr., Physics of Fully Ionized Gases (Interscience Publishers, Inc., New York, 1955).

10. D. C. Kelly, Phys. Rev. 119, 27 (1960).

11. L. Oster, Revs. Modern Phys. 32, 141 (1960).

12. L. Spitzer, Jr., Phys. Fluids 3, 659 (1960).

10. DISAPPEARANCE OF ELECTRIC CURRENT PERPENDICULAR TO THE MAGNETIC FIELD IN PLASMA

There will be no electric current inside a magnetized plasma under the following conditions:

(a) Plasma completely ionized;

(b) No anisotropy in space;

(c) Electric field perpendicular to the magnetic field;

(d) No time dependence; and

(e) No external force other than the electric field.

Spitzer's (1) equation, for a steady state, is $\nabla p = j \times B - \rho \nabla \phi$. By assumptions (b) and (e), $0 = j \times B$, hence the current perpendicular to the magnetic field must be zero. This is rigorously true, but it does not appear to follow naturally from the derivations of Cowling (2) and Chandrasekhar (3). In order to avoid any ambiguity, we present a simple interpretation.

Consider, for instance, Cowling's formulation (4). His hydromagnetic equations, which are applicable if neutral particles are present, are

$$\rho \frac{d\vec{v}}{dt} = \rho g - \text{grad } p + j \times H \tag{1}$$

$$(1-F)\,\rho \frac{d\vec{v}}{dt} = (1-F)\,\rho \vec{g} - \text{grad}\,(p_i+p_e) + \vec{j} \times \vec{H} + \kappa_e H\vec{j} - (\kappa_e+\kappa_i)\frac{1}{F} H\vec{j}_i \tag{2}$$

In these equations, F is a fraction of neutral density, ρ is total density, g is gravitational force and

$$\kappa_e = \frac{\nu_{en}}{\omega_e}, \quad \kappa_i = \frac{\nu_{in}}{\omega_i}$$

where ν_{en} is the electron neutral collision frequency, ν_{in} is the ion neutral collision frequency, and ω_e and ω_i are the cyclotron frequencies of both species.

In case the neutral density approaches zero, the limit must be taken carefully.

Cowling let all numbers F, κ_e, and κ_i go to zero and kept the ratio finite. In Eq. 2, the limiting process gives

$$\rho \frac{d\vec{v}}{dt} = \rho\vec{g} - \text{grad}\,(p_e+p_i) + \vec{j} \times \vec{H} - \left(\lim \frac{\kappa_e + \kappa_i}{F}\right) H\vec{j}_i$$

Considering

$$\frac{\vec{j}_i}{F} = ne\frac{\vec{v}_i}{F} = ne\vec{v}_n \text{ (neutral velocity)}$$

we are led to the conclusion that neutral-particle velocity must stay finite even if neutral density tends to zero. Hence Eq. 2 becomes Eq. 1. But if, as Cowling did, we make $(\kappa_e+\kappa_i)$ F nonzero, the subtraction of Eq. 1 from Eq. 2 yields

$$\lim\left(\frac{\kappa_e + \kappa_i}{F}\right) H\vec{j}_i = 0 \qquad \lim \frac{\kappa_e + \kappa_i}{F} \neq 0$$

Hence j_i becomes zero. Then Cowling's result follows.

S. Yoshikawa

References

1. L. Spitzer, Jr., Physics of Fully Ionized Gases (Interscience Publishers, Inc., New York, 1955), see Eq. (2-21).

2. T. G. Cowling, Magnetohydrodynamics (Interscience Publishers, Inc., New York, 1957).

3. S. Chandrasekhar, Plasma Physics, edited by S. K. Trehau (University of Chicago Press, Chicago, Illinois, 1960).

4. T. G. Cowling, M. N. Roy. Astron. Soc. 116, 114 (1956), see especially Eqs. (9) and (23).

II-C. PLASMA MAGNETOHYDRODYNAMICS AND ENERGY CONVERSION

Prof. E. N. Carabateas
Prof. J. A. Fay
Prof. G. N. Hatsopoulos
Prof. W. D. Jackson
Prof. H. P. Meissner
Prof. D. C. Pridmore-Brown
Prof. A. H. Shapiro
Prof. H. H. Woodson
A. W. Angelbeck
G. W. Bukow
L. Y. Cooper
R. S. Cooper
D. M. Dix
D. A. East
W. H. Heiser
E. D. Hoag
S. A. Khayatt
G. B. Kliman
P. Klimowski
A. Kniazzeh
M. F. Koskinen
A. T. Lewis
J. R. Melcher
W. T. Norris*
J. K. Oddson
J. P. Penhune
E. S. Pierson
J. W. Poduska
J. Wasserlein

RESEARCH OBJECTIVES

1. Plasma Magnetohydrodynamics†

The general purpose of the magnetohydrodynamic research is to explore interaction phenomena in those situations in which the fluid can be considered to be predominantly a continuum. This includes a wide range of phenomena, from the flow of liquid metals through magnetic fields to the propagation of hydromagnetic shock waves. At the present time, we are exploring such problems as boundary-layer flow over a flat plate with normal magnetic field, the flow over pitot tubes in the presence of a magnetic field, the confinement of dense plasmas with dc and ac magnetic fields, the acceleration of plasmas by $J \times B$ forces, and the propagation of disturbances in a medium containing a magnetic field.

While some of the experimental work is concerned with liquid metals, a large proportion makes use of shock tubes to produce high-velocity plasmas whose interactions with magnetic fields can be studied. One of our research objectives is to extend these techniques to include a greater range of physical parameters.

J. A. Fay

2. Energy Conversion

(a) Magnetohydrodynamic Energy Conversion‡

The objectives in this area are twofold:

(i) To study problems of magnetohydrodynamic flow in order to obtain a better understanding of the many phenomena involved, such as turbulence and wave motion. This involves both theoretical and experimental work.

(ii) To study systems in which energy conversion can occur between flow energy in a conducting liquid or gas and an electrical system. The systems of interest include steady and nonsteady fluid flow, and dc and ac electrical systems. The work involves theoretical and experimental evaluation of magnetohydrodynamic conversion schemes that have already been proposed and suggestions for new conversion schemes.

H. H. Woodson, W. D. Jackson

---

*Commonwealth Fellow from England, 1960-61.

†This work was supported in part by National Science Foundation under Grant G-9330, and in part by Contract AF19(604)-4551 with Air Force Cambridge Research Center.

‡This work was supported in part by National Science Foundation under Grant G-9330, and in part by WADD Contract AF33(616)-7624 with Flight Accessories Laboratory, Wright-Patterson Air Force Base, Ohio.

(b) Thermionic Energy Conversion*

Present objectives lie in four distinct areas of direct thermionic energy conversion. The first relates to the theoretical study of the Richardson equation by means of irreversible thermodynamics; the second, to experimental verification of the Saha-Langmuir equation in the region of partial coverage; the third, to the theoretical and experimental analysis of plasmas and sheaths; and the fourth, to the correlation of the effect of emitter work function on the efficiency and ion production rate of cesium converters while operating in the neutralized space-charge region.

G. N. Hatsopoulos, E. N. Carabateas

(c) Fuel Cells†

Our objective is to learn more about the mechanism of the various chemical, physical, and electrochemical processes that occur simultaneously in a fuel cell. Studies will be directed toward satisfying the criteria of high electrode current density and high efficiency in low-temperature, low-pressure fuel cells that are capable of operating on air and hydrogen and commonly available hydrocarbons.

H. P. Meissner

1. INDUCTION-DRIVEN MAGNETOHYDRODYNAMIC FLOW

This analysis concerns the laminar flow of a viscous, incompressible, electrically conducting fluid (for example, Hg or NaK) in a nonconducting high-aspect-ratio channel, as shown in Fig. II-26. The fluid is driven mechanically by the difference in pressure between reservoirs at the ends of the channel (the pressure gradient along the channel), and is driven electrically by the traveling magnetic field produced by a two-phase winding on the surfaces of the highly permeable pole pieces that enclose the channel. For the purposes of analysis, the exciting current is represented by sinusoidal current sheets, in the planes $y = \pm a$, of the form

$$\overline{K}(y=+a) = \bar{i}_x K_o \mathrm{Re}\, e^{i(\omega t - kz)} \tag{1}$$

$$\overline{K}(y=-a) = \pm \bar{i}_x K_o \mathrm{Re}\, e^{i(\omega t - kz)} \tag{2}$$

with the result that the traveling magnetic field has the phase velocity ω/k. If the positive sign is taken in Eq. 2, the excitation and the y component of the resulting magnetic field have even symmetry with respect to y; if the negative sign is taken, they have odd symmetry.

---

*This work was supported in part by National Science Foundation under Grant G-9330, and in part by WADD Contract AF33(616)-7624 with Flight Accessories Laboratory, Wright-Patterson Air Force Base, Ohio.

†This work was supported in part by WADD Contract AF33(616)-7624 with Flight Accessories Laboratory, Wright-Patterson Air Force Base, Ohio.

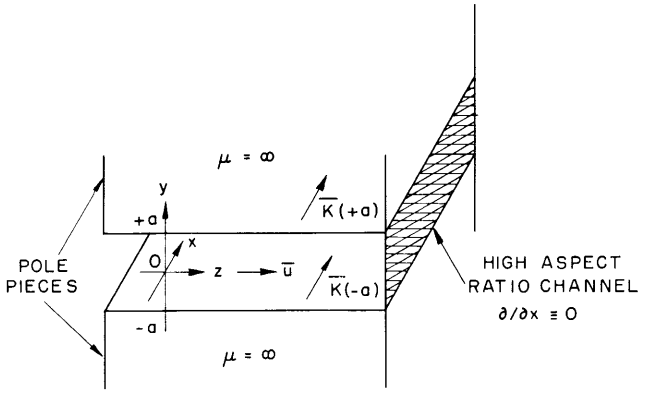

Fig. II-26. An induction-driven magnetohydrodynamic channel flow.

In general, the fluid velocity $\bar{u}$ will have both y and z components, which vary periodically with both z and t, and aperiodically with y. An important special case occurs when the density and viscosity of the fluid are sufficiently high that the time variations in the velocity field can be ignored. This case is discussed here. The normalized velocity is assumed to be of the form

$$\bar{u} = \bar{i}_z u(\hat{y}) \tag{3}$$

while the normalized magnetic field is given by

$$\bar{h} = \mathrm{Re}\left\{\left[\bar{i}_y \underline{h}_y(\hat{y}) + \bar{i}_z \underline{h}_z(\hat{y})\right] e^{i\alpha(\tau-\hat{z})}\right\} \tag{4}$$

in which $\hat{x}$, $\hat{y}$, and $\hat{z}$ are the coordinates normalized with respect to the channel half-width a, the normalized time is $\tau = \omega t/a$, and the parameter $\alpha = ka$ measures the ratio of the channel half-width to the excitation pole spacing. When Eqs. 3 and 4 are substituted in the magnetohydrodynamic field and force equations, the following pair of nonlinear, coupled, ordinarily differential equations results:

$$\frac{d^2\underline{h}_y}{d\hat{y}^2} - \alpha^2\left(1 + i\frac{R_m}{\alpha}\epsilon_z\right)\underline{h}_y = 0 \tag{5}$$

$$\frac{d^2\epsilon_z}{d\hat{y}^2} - \frac{1}{2}M^2\underline{h}_y\underline{h}_y^*\epsilon_z = -RP_o \tag{6}$$

In Eqs. 5 and 6, $\epsilon_z = 1 - u_z$ is the velocity defect, $R_m/\alpha = \sigma\mu_o\omega/k^2$ is the magnetic Reynolds number, $M = \mu_o K_o a(\sigma/\eta)^{1/2}$ is the Hartmann number, $R = \rho\omega a/k\eta$ is the hydraulic Reynolds number, and $P_o = \left\langle \frac{\partial p}{\partial \hat{z}} \right\rangle$ is the time average of the pressure gradient in the z-direction.

Harris (1) obtained equations similar to Eqs. 5 and 6, and showed that under the drastic simplification, $|a^2(1+iR_m/a)| \ll 1$, $\underline{h}_y$ is a constant, and Eq. 6 is linear and yields velocity profiles similar to those in Hartmann flow (2). The present study is concerned with obtaining general solutions to the original nonlinear equations, Eqs. 5 and 6. The technique employed is that of making a perturbation expansion in the parameter R_m/a,

$$\underline{h}_y = \sum_{n=0}^{\infty} \underline{h}_{yn}\left(\frac{R_m}{a}\right)^n \tag{7}$$

$$\epsilon_z = \sum_{n=0}^{\infty} \epsilon_{zn}\left(\frac{R_m}{a}\right)^n \tag{8}$$

This expansion is appealing from a physical viewpoint, because R_m/a is usually small. The substitution of the series Eqs. 7 and 8 in Eqs. 5 and 6 yields simple linear differential equations for the zero-order magnetic field and velocity defect,

$$\frac{d^2\underline{h}_{yo}}{d\hat{y}^2} - a^2\underline{h}_{yo} = 0 \tag{9}$$

$$\frac{d^2\epsilon_{zo}}{d\hat{y}^2} - \frac{1}{2}M^2\underline{h}_{yo}\underline{h}^*_{yo}\epsilon_{zo} = -RP_o \tag{10}$$

The solutions of Eq. 9, subject to the boundary conditions imposed by the excitation surface currents and the highly permeable pole pieces, are $\underline{h}_{yo} = -i \cosh a\hat{y}/\sinh a$ for even excitation, and $\underline{h}_{yo} = -i \sinh a\hat{y}/\cosh a$ for odd excitation. If these magnetic-field solutions are substituted in Eq. 10, the equation for the zero-order velocity defect has the form of an inhomogeneous modified Mathieu equation. Relatively little theoretical work has been done on this type of Mathieu equation, and none has thus far been discovered that is particularly helpful in this particular problem. For this reason, homogeneous and particular solutions to Eq. 10, for various values of the parameters M and a, have been integrated numerically on the IBM 709 digital computer (3). A typical set of velocity profiles obtained from these calculations is shown in Fig. II-27. The excitation is even, $a = 1.0$, $M = 10.0$, and the pressure drive RP_o is varied so that the center channel velocity varies from twice the traveling-wave speed to minus the traveling-wave speed. When RP_o is positive, the device is a pump; when it is negative, the amount of power loss determines whether it is a flow damper or a generator. The important feature of these velocity profiles is that they do not all have the same shape as the Hartmann profiles do, but clearly show the effect of the fact that the electromagnetic force is stronger near the channel walls than at the center, while the pressure

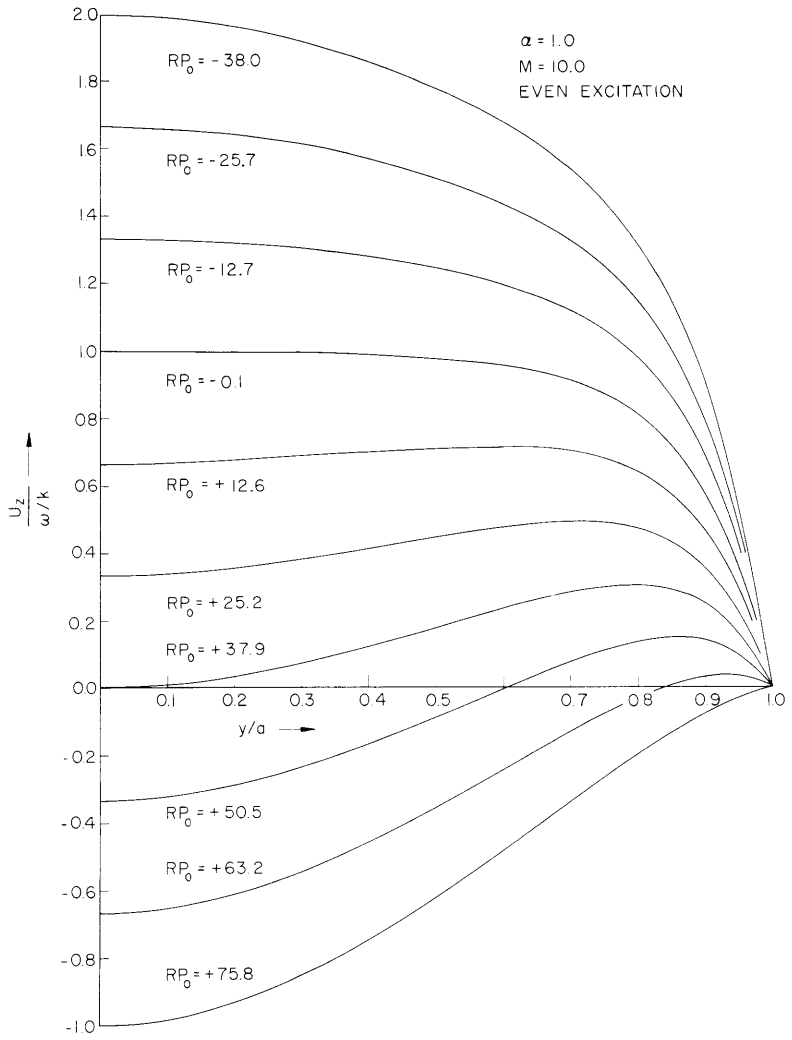

Fig. II-27. Typical velocity profiles in laminar, induction-driven magnetohydrodynamic flow.

force is uniform. In fact, in some of the profiles the fluid is moving in one direction near the channel walls, but in the opposite direction at the center. Such profiles are probably more inclined to instability than others, since they possess a point of inflection.

The first-order velocity defect in the series Eq. 8 can be shown to be zero, with the result that the error in the velocity profiles shown in Fig. II-27 is second-order in R_m/a. At present, the first-order and second-order magnetic fields, and the second-order velocity defect are being computed, and the general case in which the fluid velocity has components that vary with time is being analyzed.

J. P. Penhune

References

1. L. P. Harris, Hydromagnetic Channel Flows (The Technology Press of Massachusetts Institute of Technology, Cambridge, Mass., and John Wiley and Sons, Inc., New York, 1960), see Chapter 8.

2. T. G. Cowling, Magnetohydrodynamics (Interscience Publishers, Inc., New York, 1957), see Section 1.5.

3. This computation was performed at the Computation Center, M. I. T.